Laser-hybrid Accelerator for Radiobiological Applications (LhARA)

John Adams Institute Accelerator Design Project 2024

M. Pereira, G. Passarelli
Royal Holloway, University of London

C. Jolly, S. Leadley, C. Lehmann, S. Preston
University of Oxford

G. Christian, L. Bradley, J. Hills, L. Kennedy
Imperial College London

Motivation

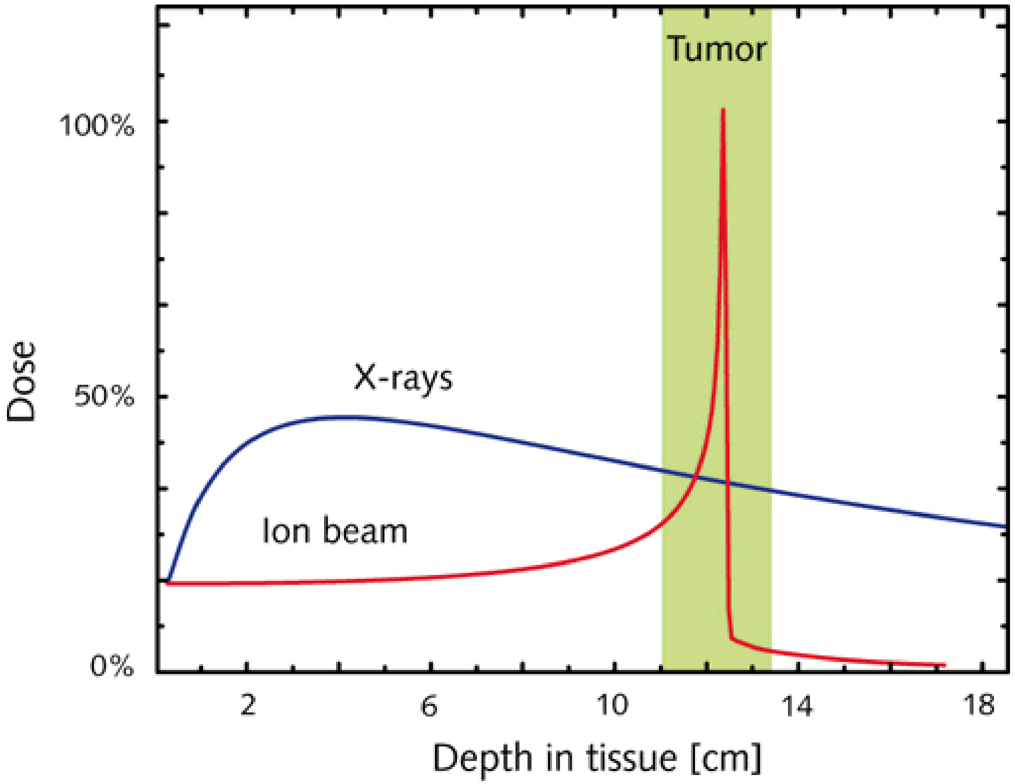

[1] Comparison of radiation dose as a function of depth.

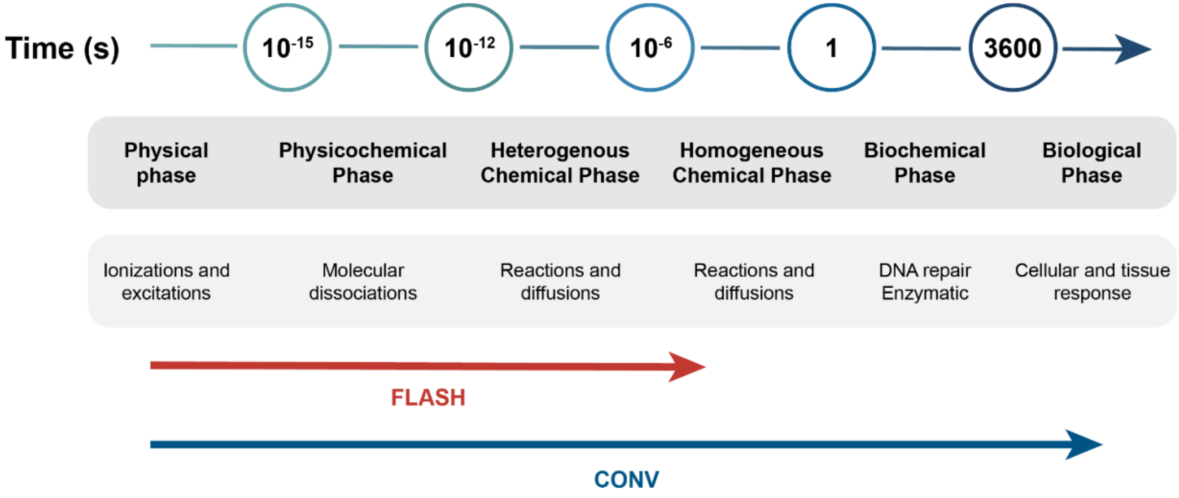

[2] Flash timescales compared to conventional RT

- Development of more accessible, cheaper alternatives for RT (radiation therapy)
- Study of ion beam radiobiology
- Exploration of novel treatment modalities

Introduction

LhARA (Laser-hybrid accelerator for radiobiological applications)

Beam Parameters

- Energy
- Ion species
- Dose, dose spatial distribution, dose rate
- Biological end point

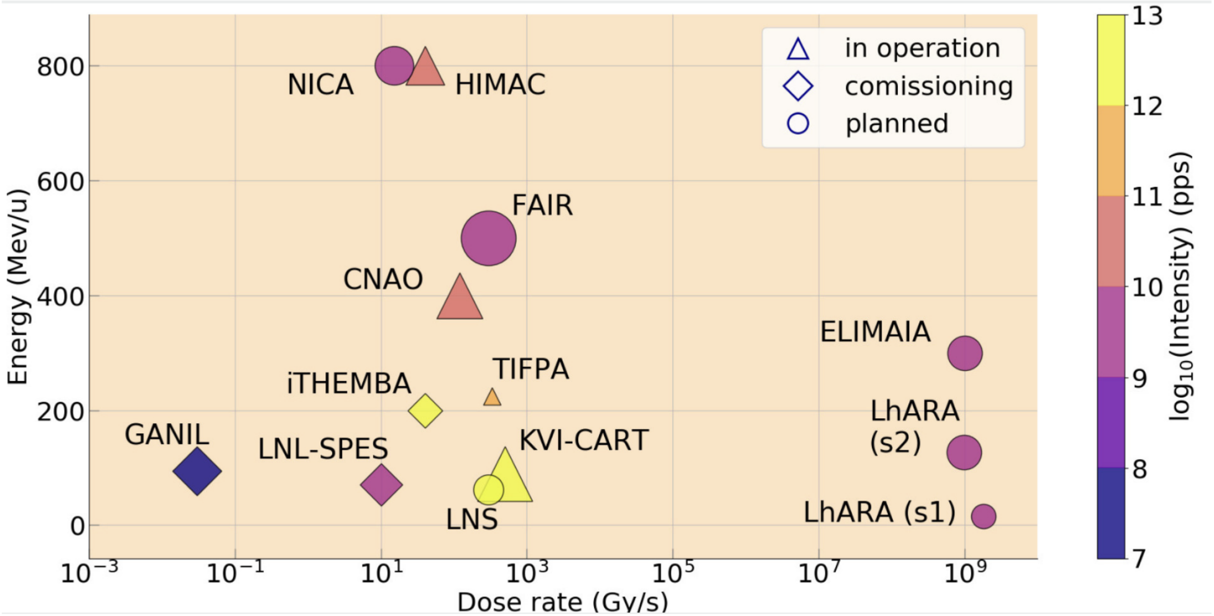

[3] Facility comparison showing where the planned LhARA S1 & S2 are in energy & dose rate.

Introduction

Target Normal Sheath Acceleration (TNSA): Exploration of Hybrid Acceleration

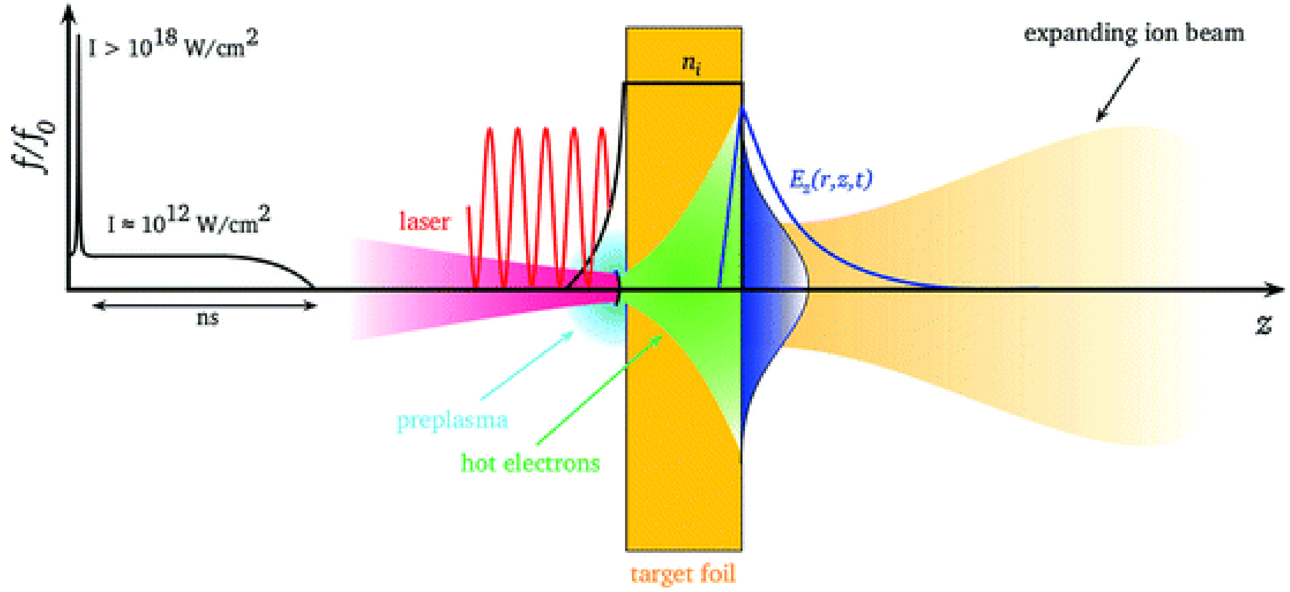

[4] Solid target interaction using TNSA to produce proton beams

Parameter	Value or range	Unit
Laser power	100	TW
Laser energy	2.5	J
Laser pulse length	25	fs
Laser rep. rate	10	Hz
Proton energy	15	MeV

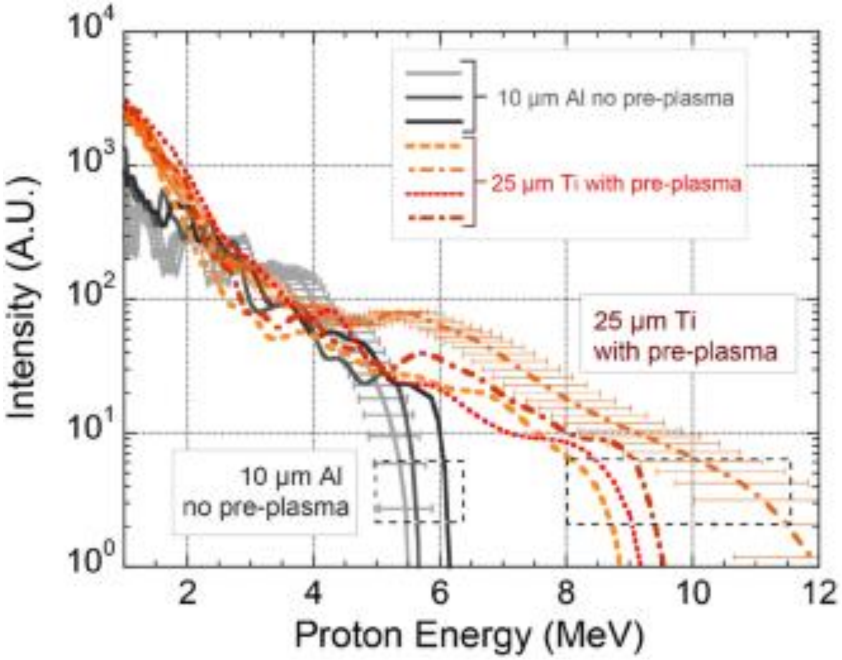

[5] Ion beam spectra characteristics

Gabor Lenses

Advantages

- More efficient focusing compared to high-field solenoid
- Reduces costs
- Focus in both planes simultaneously
- Variable focusing strength proportional to plasma density

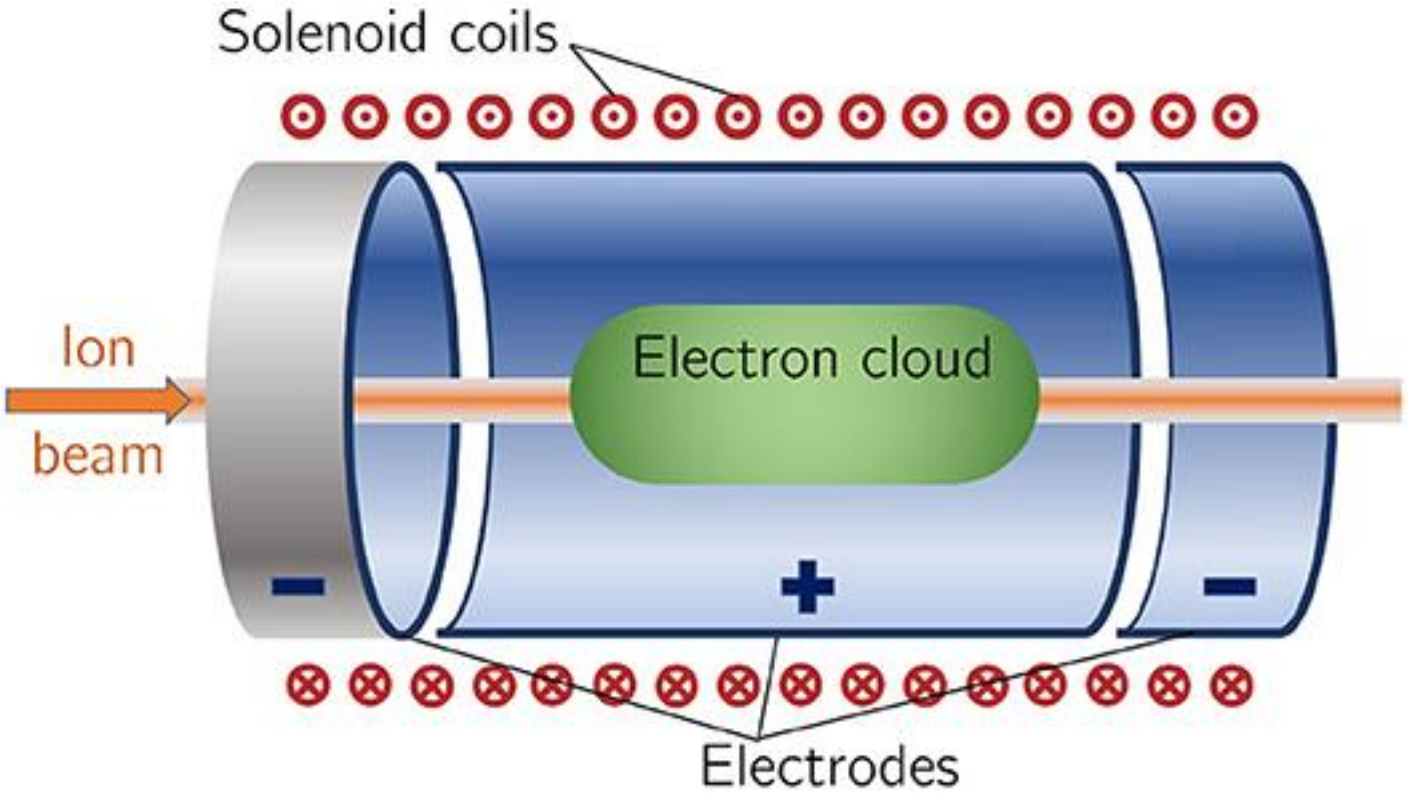

[6] Schematic of Gabor Lens to be used in LhARA

LhARA Design Overview

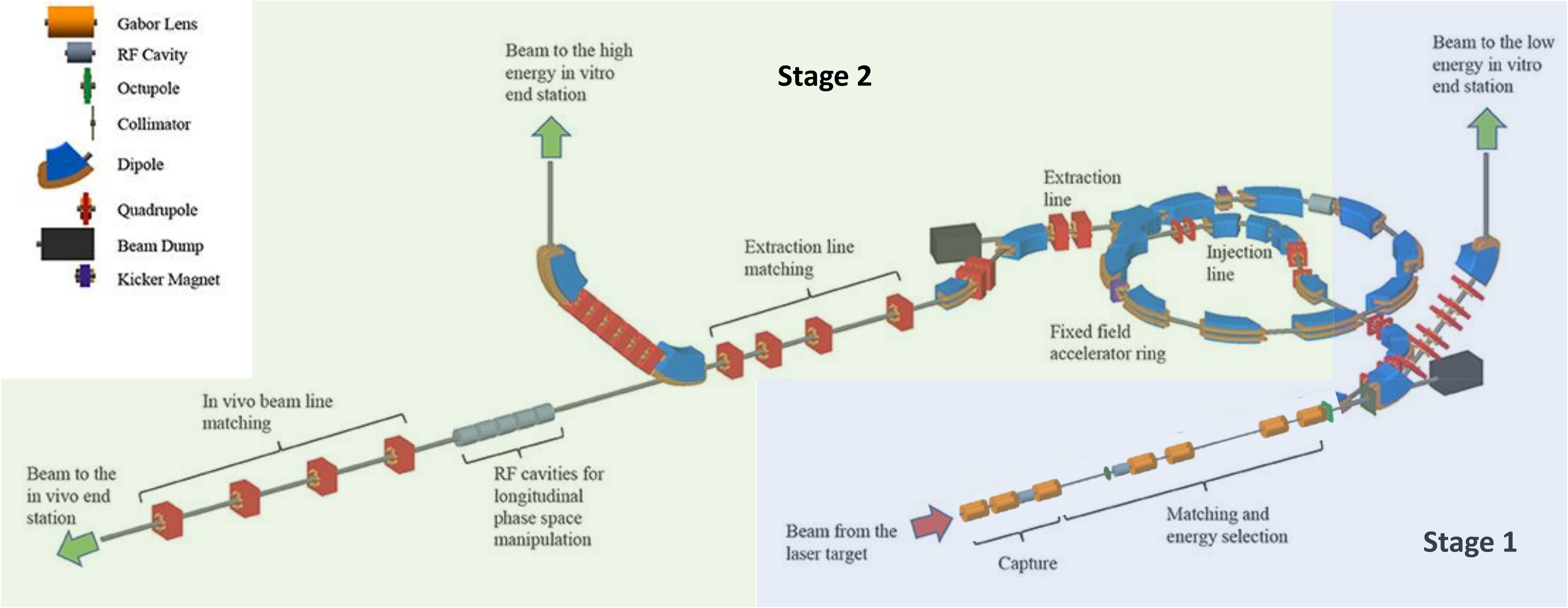

[7] Proposed LhARA facility.

End Station Specifications

Low energy (in vitro)

1. Low uniform dose distribution (<5%)
2. Minimal beam losses
3. Maximized dose delivery
4. Maximum diameter 1-3cm or focused down to 1mm
5. 12-15 MeV

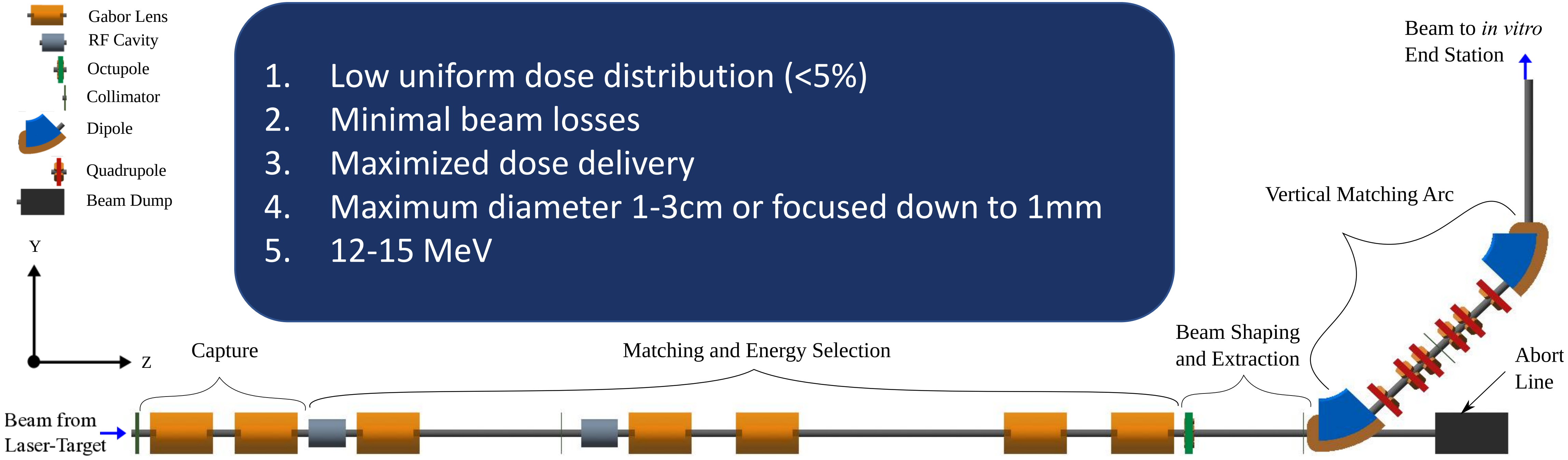

High energy (in vivo and in vitro)

1. Variable Injection energy using stage 1 beam line focusing strengths allows variable proton energies
2. 15 MeV -127 MeV

Lattice Design

Gregory Christian (gregory.christian.22@imperial.ac.uk)
Imperial College London
Jasmin Hills (jasmin.hills19@imperial.ac.uk)
Imperial College London
Lewis Kennedy (l.kennedy23@imperial.ac.uk)
Imperial College London
Matt Pereira (matthew.pereira.2023@live.rhul.ac.uk)
Royal Holloway, University of London
Shaun Preston (shaun.preston@physics.ox.ac.uk)
University of Oxford

Lattice Constraints

1. Beam focus after Lens 3 (S = 5.5m)
2. Twiss alpha -> 0 between Gabor lenses 2-3
3. High dispersion and low Twiss beta in the arc
4. Twiss alpha and dispersion -> 0 at end station
5. Low twiss beta (spot size)

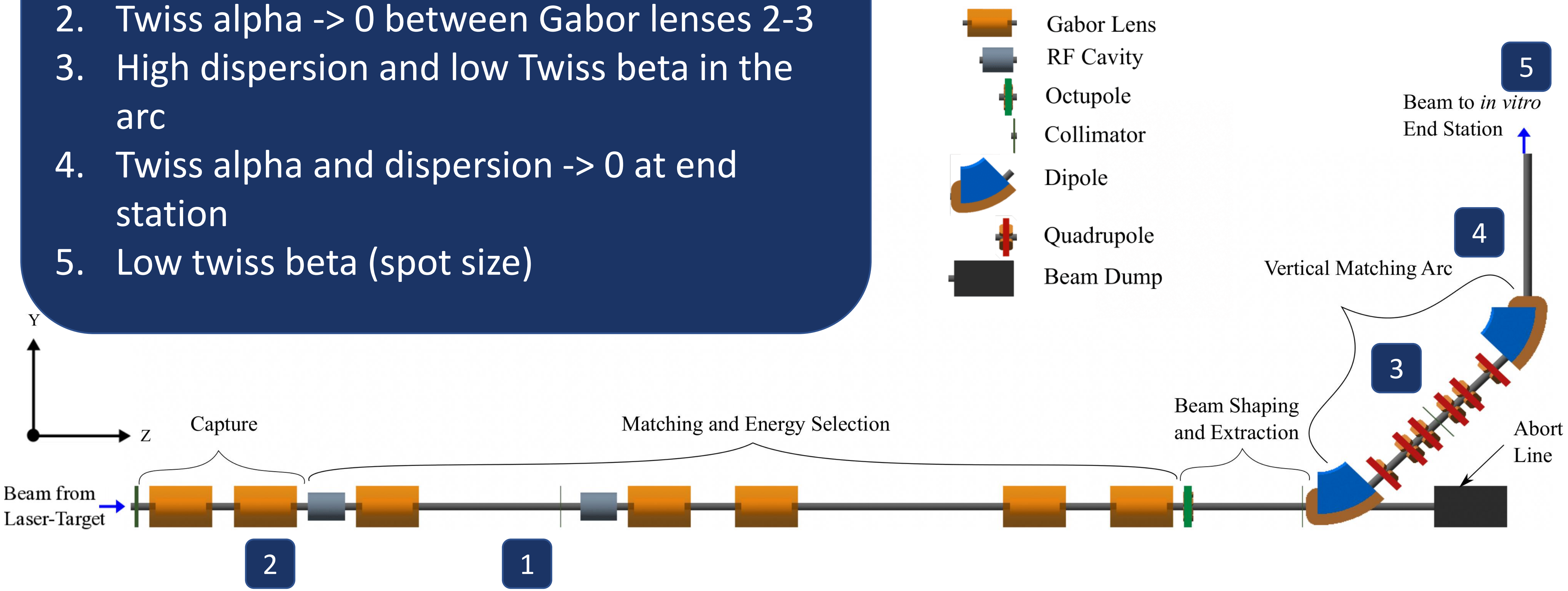

Lattice

Beam Size Optimisation – 3.0cm Configuration

Methodical Accelerator Design (MAD-X)

- General purpose accelerator design tool with a focus on beam dynamics and optics optimisation

1. Beam focus after Lens 3 (S = 5.5m)
2. Twiss alpha -> 0 between Gabor lenses 2-3
3. High dispersion and low Twiss beta in the arc
4. Twiss alpha and dispersion -> 0 at end station

To keep constraint 1 satisfied for all configurations, only lenses 4-6 were varied to achieve smaller spot sizes.

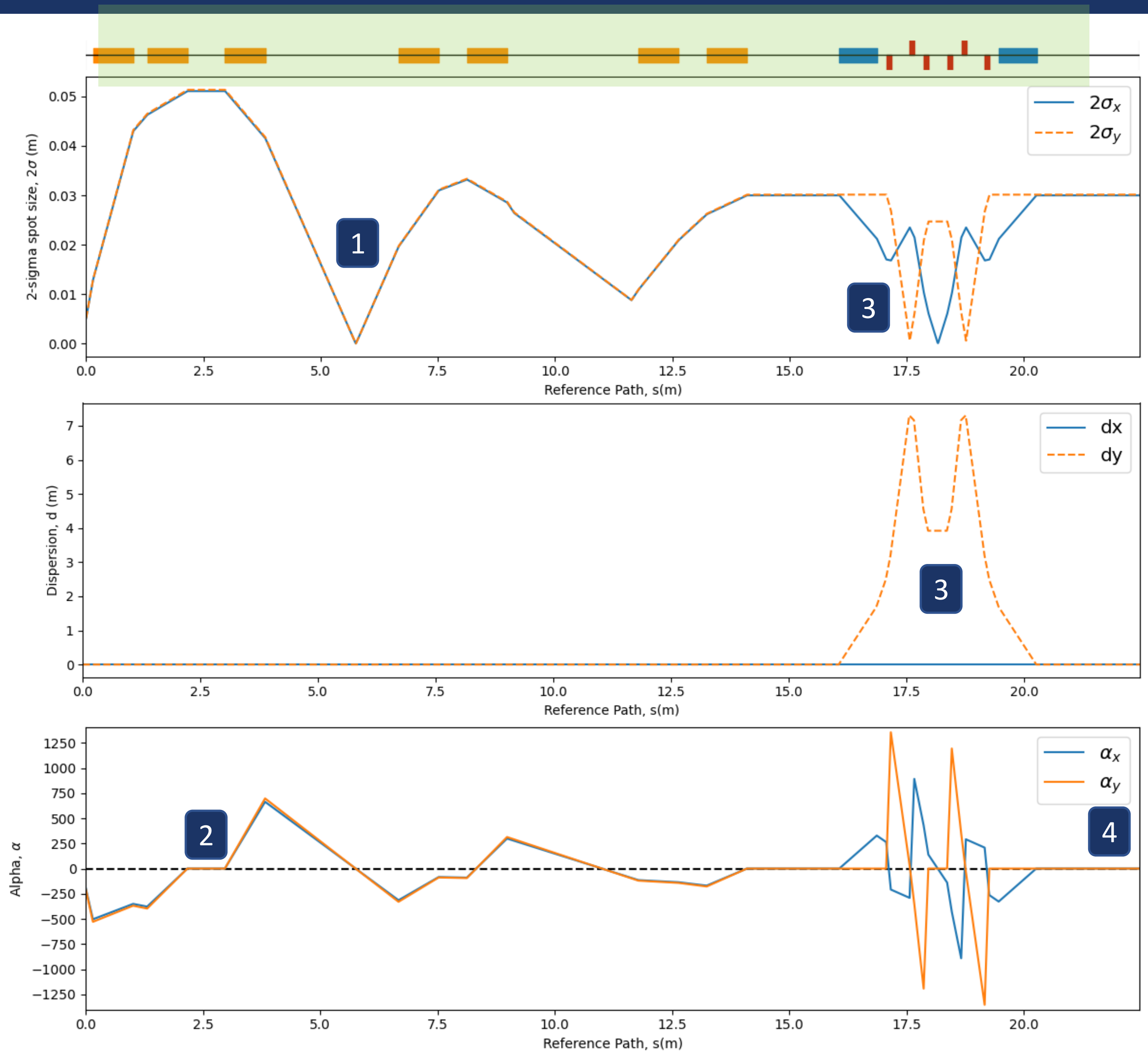

Lattice

Beam Size Optimisation – MAD-X Solenoid Matching

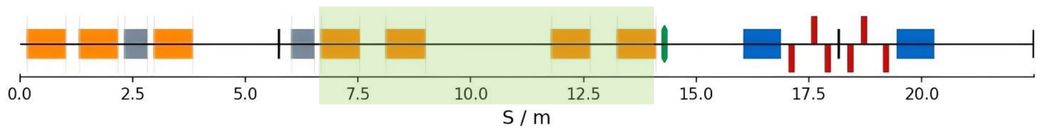

MATCH module used to vary solenoid strengths and apply lattice constraints to find lower spot size configurations

	Solenoid Strength, K_S			
2σ Spot Size (cm)	Lens 4	Lens 5	Lens 6	Lens 7
3.0	1.80	1.61	1.24	1.91
2.0	1.94	1.48	1.82	0.65
1.0	1.93	1.33	2.49	0.88

Beyond 1.0 cm, MAD-X is unable to accurately reach the intended beam size AND sufficiently satisfy lattice constraints in Dispersion and Twiss Alpha

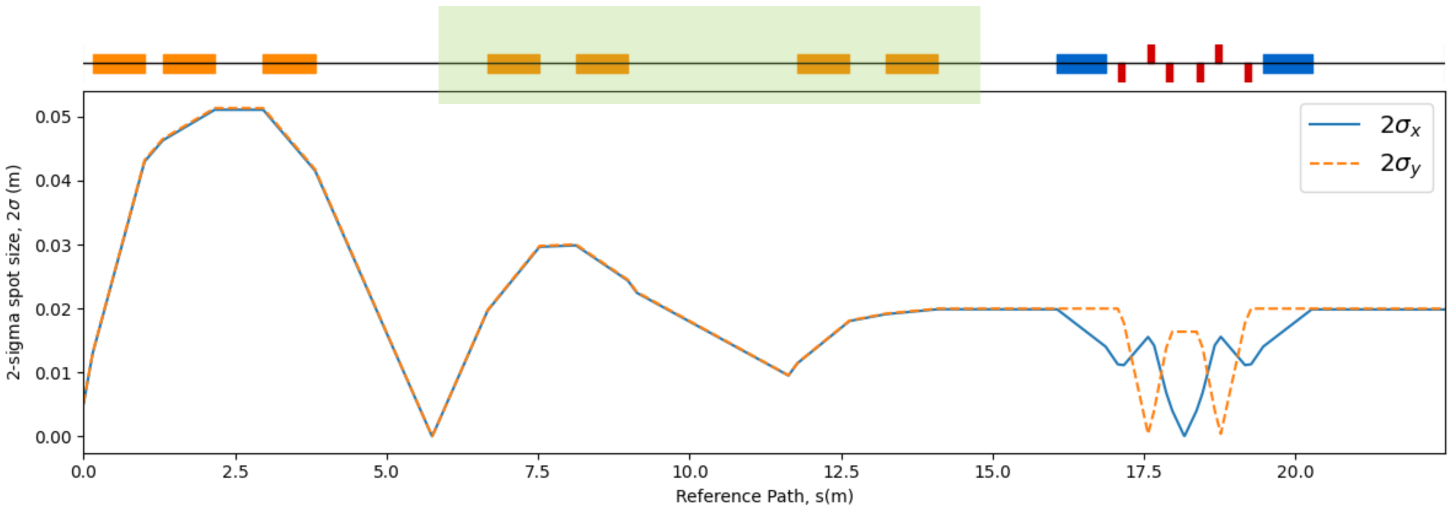

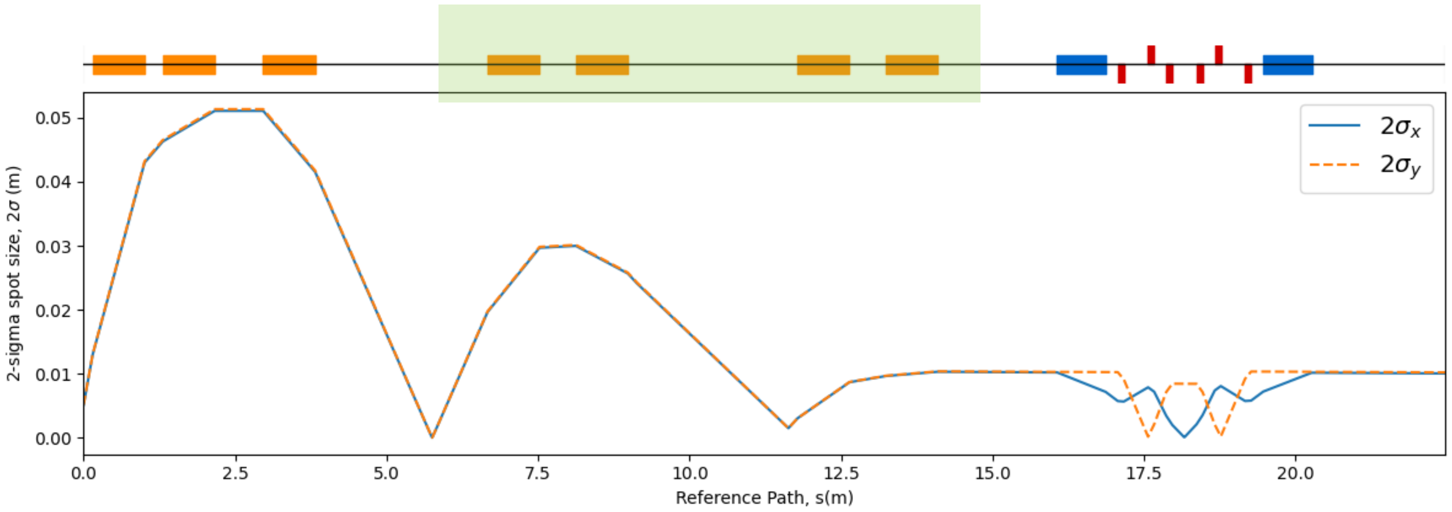

Lattice

Arc Optimisation - Quadrupole Strength

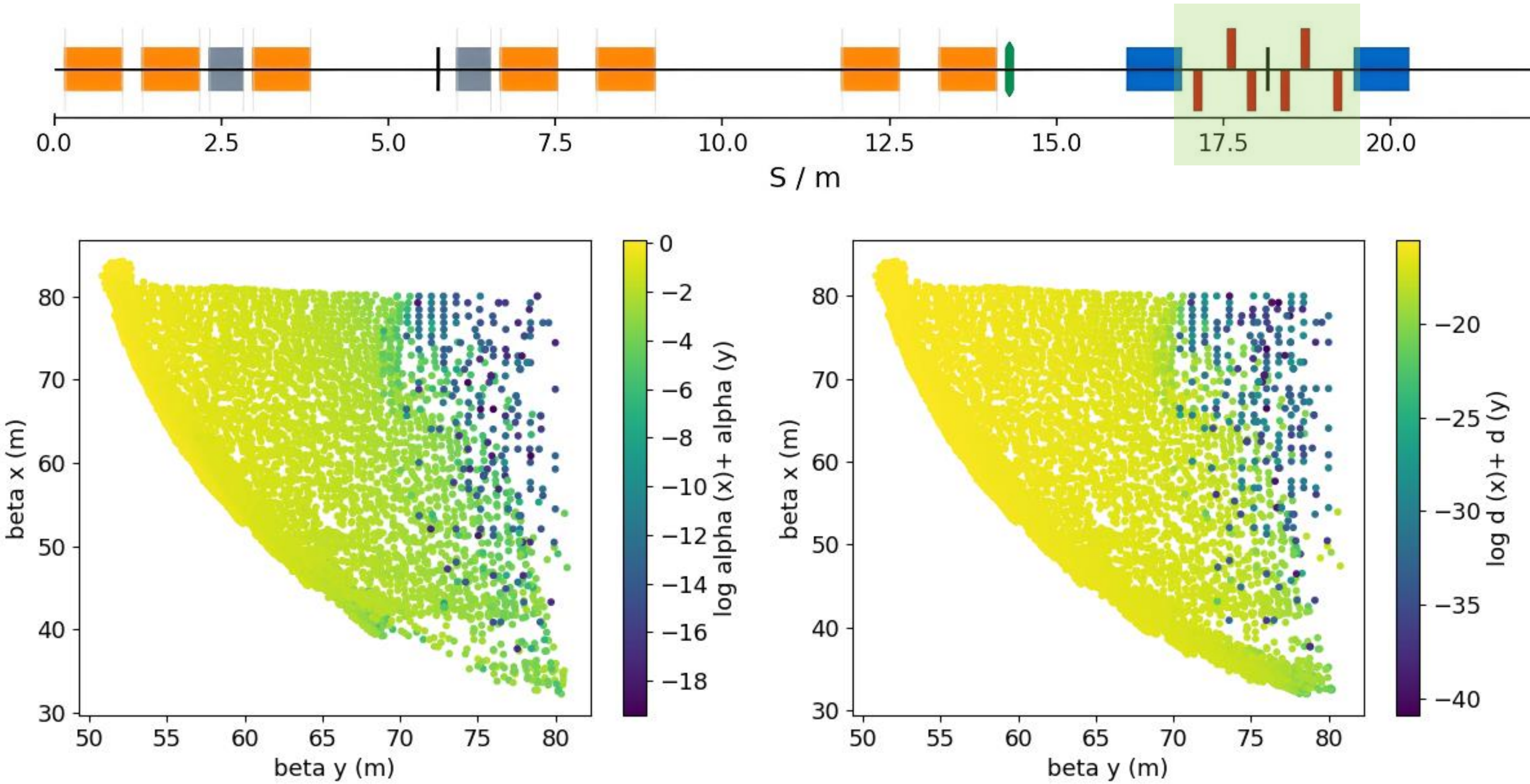

Alpha and dispersion for a variety of beta values

Required strengths: -21.9, 31.2, -32, -31.1,31.5, -23.3 [1/m]

Lattice

BDSIM Lattice Model

Beam Delivery Simulation (BDSIM)

- Program utilising the Geant4 physics libraries to simulate the transport of a particle beam through a 3D model of the accelerator with realistic physics processes.

Beam Delivery Simulation

[8]

Studies on the BDSIM Lattice

- Energy loss and deposition along the beamline
- Dose rate calculations
- Beam uniformity through the octupole
- Gabor lens performance study (vs solenoids)
- Tracking through a 3D field map of the student designed RF cavity.

Studies on the BDSIM lattice use a 3.0 cm beam size to account for:

- BDSIM not including the effects of space charge
- The largest beam size being most effective for studying losses

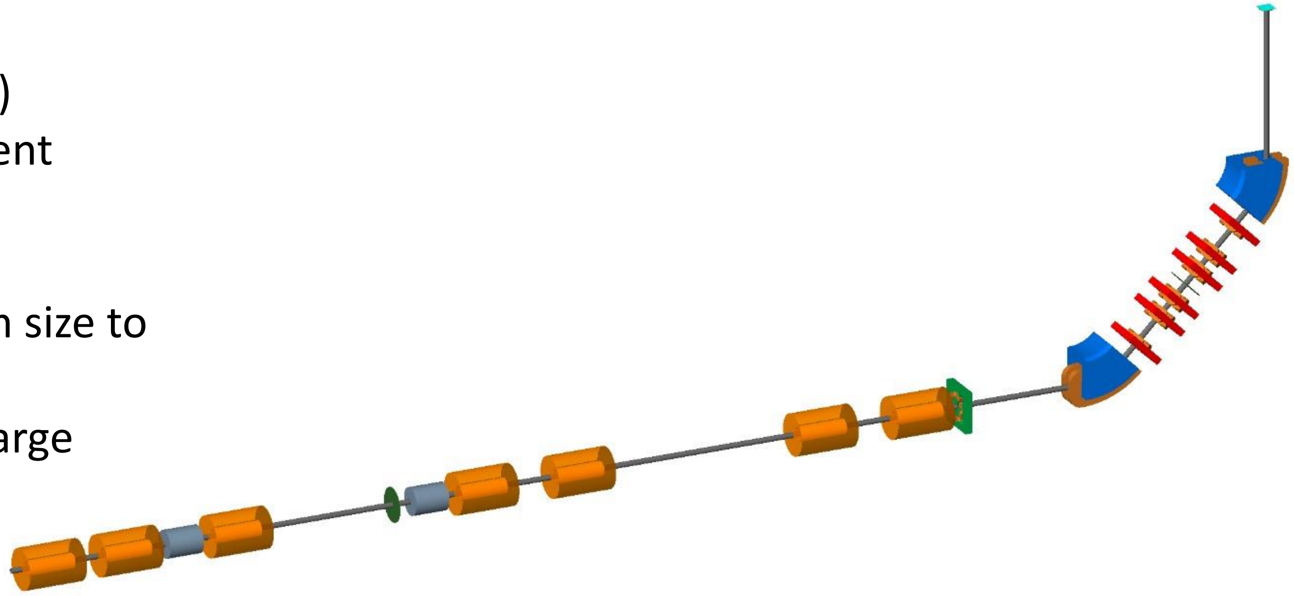

Beam and Energy Loss

Solenoid run with 10000 protons excluding collimators

A Global aperture radius of 3.65cm was found to minimize total beam loss across the lattice.

The "g4QGSP_BIC_EMZ" Geant4 physics list was used for simulation. Chosen as it is most common for handling physics for radiobiology/medical applications.

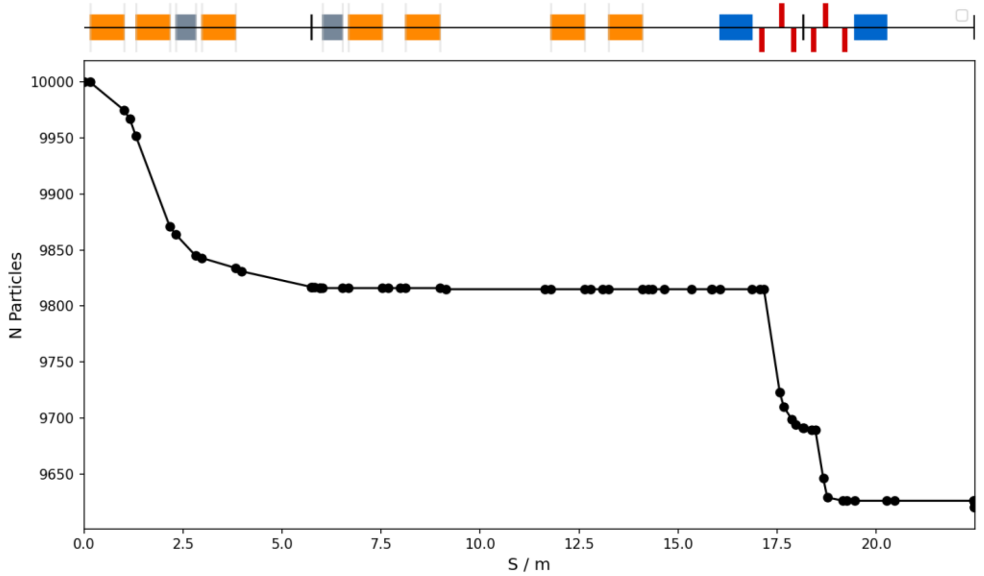

Energy and Deposition plot under the same conditions with 10 million protons.

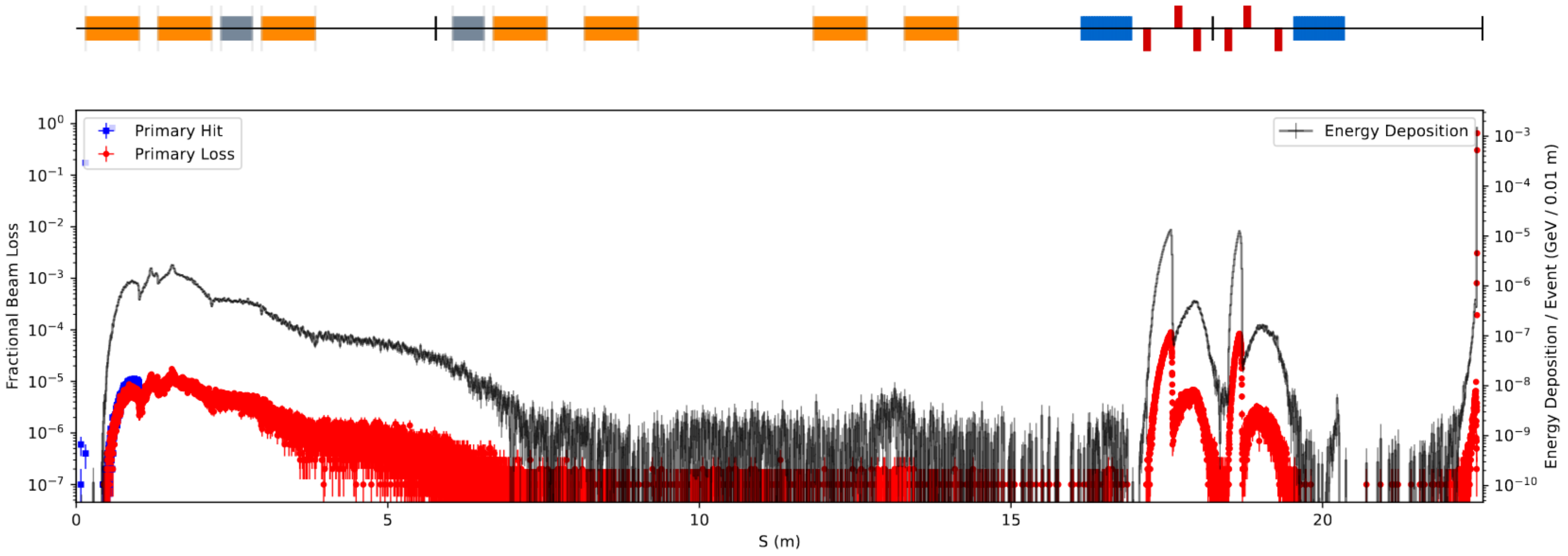

Lattice

Beam and Energy Loss

Collimator 1 – After GL3
- **Energy Cleaning**
- Positioned where the beam is at its smallest
- Circular aperture
    - Radius of 1.8mm (~2σ)

Collimator 2 – Middle of Vertical Arc
- **Momentum Cleaning**
- At the point of maximum Dispersion
- Elliptical aperture
    - Y-width of 1.2cm (~2σ)
    - X-width of 2.0cm
- Particles lost in dispersive y-axis, minimal losses in x.

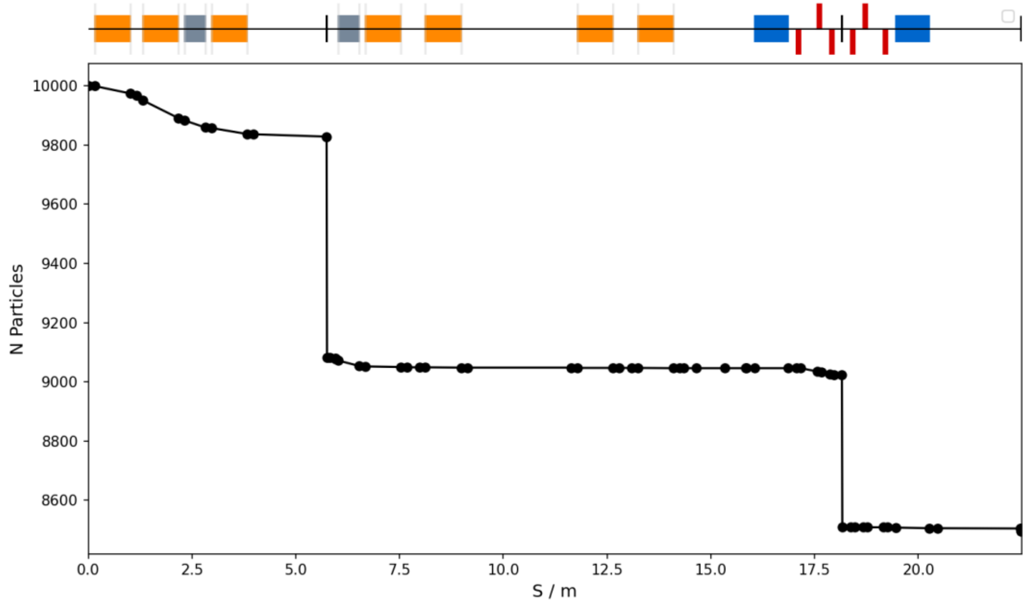

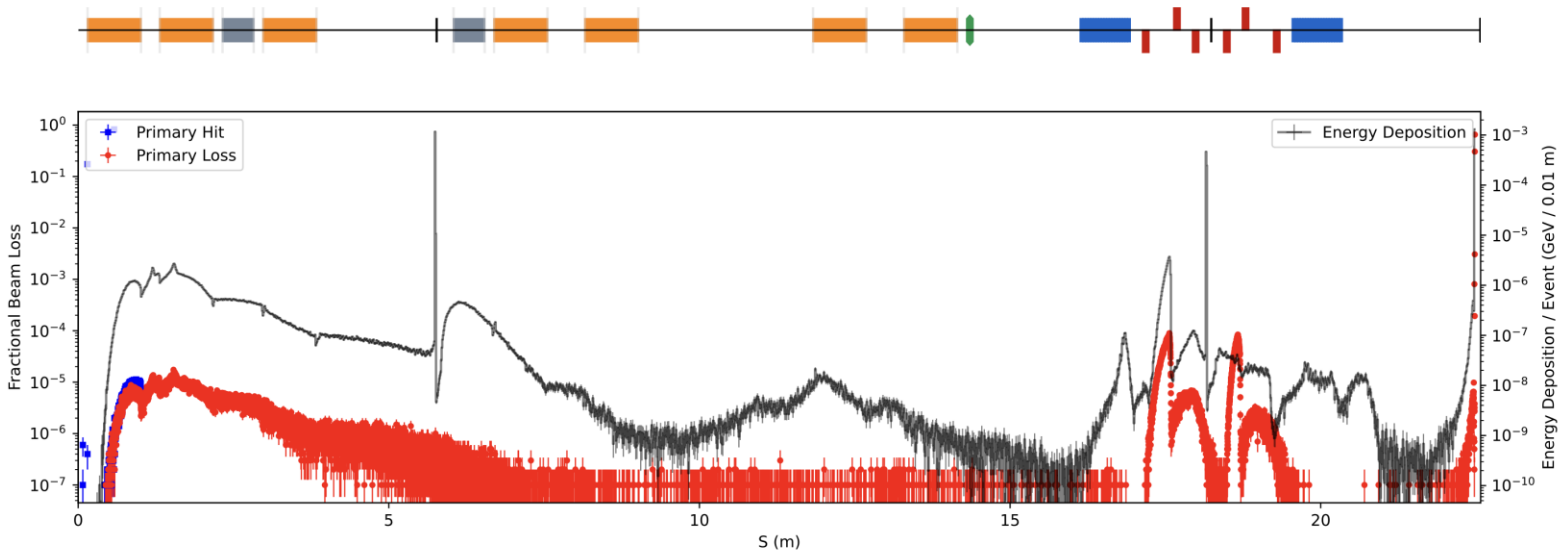

Stage 1 End Station Dosimetry in BDSIM

To enable **Dose Calculation**, a model end station target is placed at the end of the stage 1 lattice.

Vacuum Window – 75 µm of mylar

Scintillation Fibre - 250µm of polystyrene

Air Gap – 5 mm

Container – 1.3mm of polystyrene

Water – 2.4mm

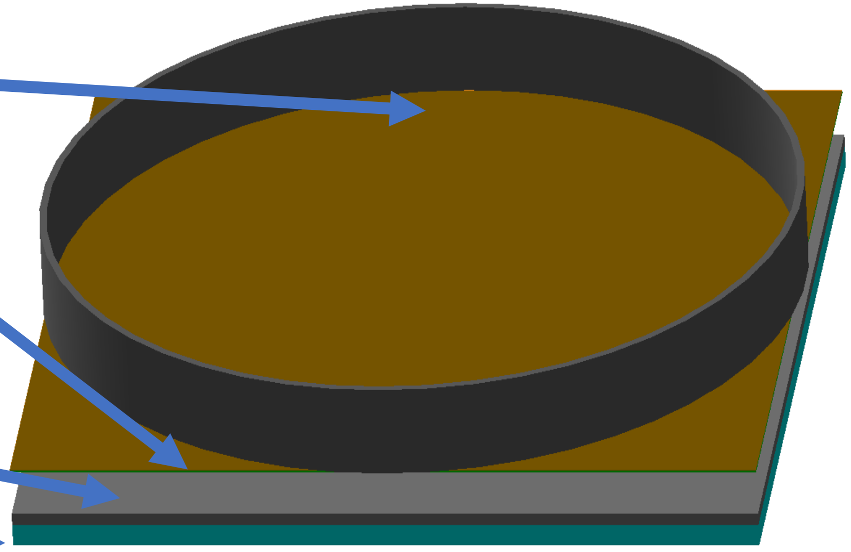

Dose is scored in a cylindrical volume within the water comparable to a Markus ion chamber

r = 2.65 mm

Dose Rate for 1cm beam directly into end station (no losses) = 122.63 ± 1.41 Gy/s
Close to LhARA's theoretical maximum dose rate in literature (~120 Gy/s) [7]

Lattice

Dose Rate Calculation

Dose Rate Calculation:

- Dose per proton extracted from the scorer and scaled by a factor of 10^{10} to represent the expected 10^{9} particles per shot and the 10 Hz repetition rate of the laser
- Large errors due to small sample size compared with the real number of expected particles per shot

	Dose Rate (Gy/s)	Change w.r.t Reference (Gy/s)	Within Error of Reference?
Reference	16.92 ± 0.61	n/a	n/a
3.65cm Aperture	17.23 ± 0.61	+ 0.31	Yes
w/ Collimator 1	17.51 ± 0.62	+ 0.59	Yes
w/ Collimator 1+2	14.78 ± 0.57	-2.14	No

Significant impact of the second, **Momentum Cleaning**, collimator on the dose rate validates the motivation for LhARA's smaller beam sizes.

Smaller beams will experience less loss in that second collimator and therefore correlate to a higher dose at the end station.

Beam Uniformity - Octupole Tracking

Why?

*We desire a **uniform** beam at the end station to provide a spatially consistent dose to the entire target.*

How?

*Octupoles! Spatial flattening of the distribution is captured via **kurtosis**.*

Definition:

$$\mu_4 = \mathbb{E}\left[\frac{(x - \mu_x)^4}{\sigma_x^4}\right]$$

using scipy stats

So … how can we measure success?

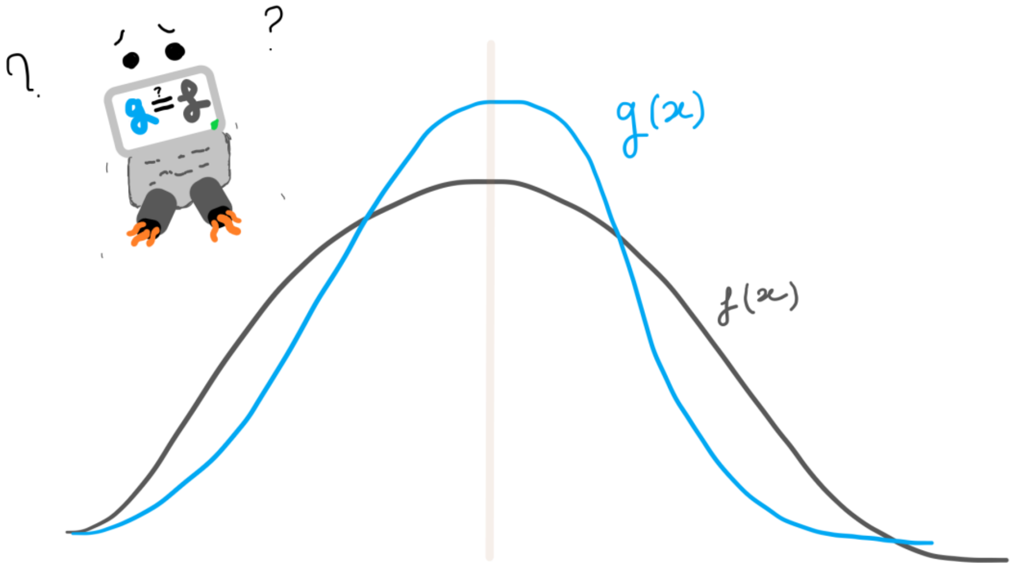

Gaussian: μ = 3

Perfectly Flat: μ = 1

Let's define a flatness threshold!

Octupole Tracking – Beam Transfer through Stage 1

10,000 particles through the beamline ...

Octupole ***Selection Arc***

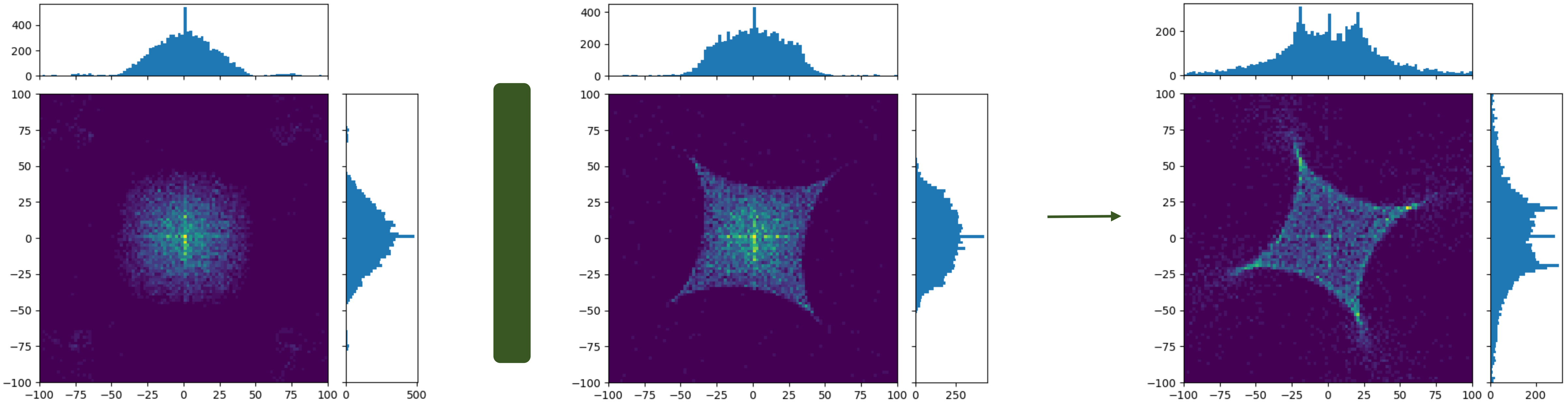

Lattice

Octupole Tracking – Quantifying Flatness

This is useful, but it's not entirely clear how we can measure the kurtosis of the beam distribution ….

*We can **rotate** the beam post-mortem in code and get an accurate figure for the uniform width.*

Kurtosis metric of 1.73 (Non-Fisher)

We can expect a largely uniform coverage of the end station target.

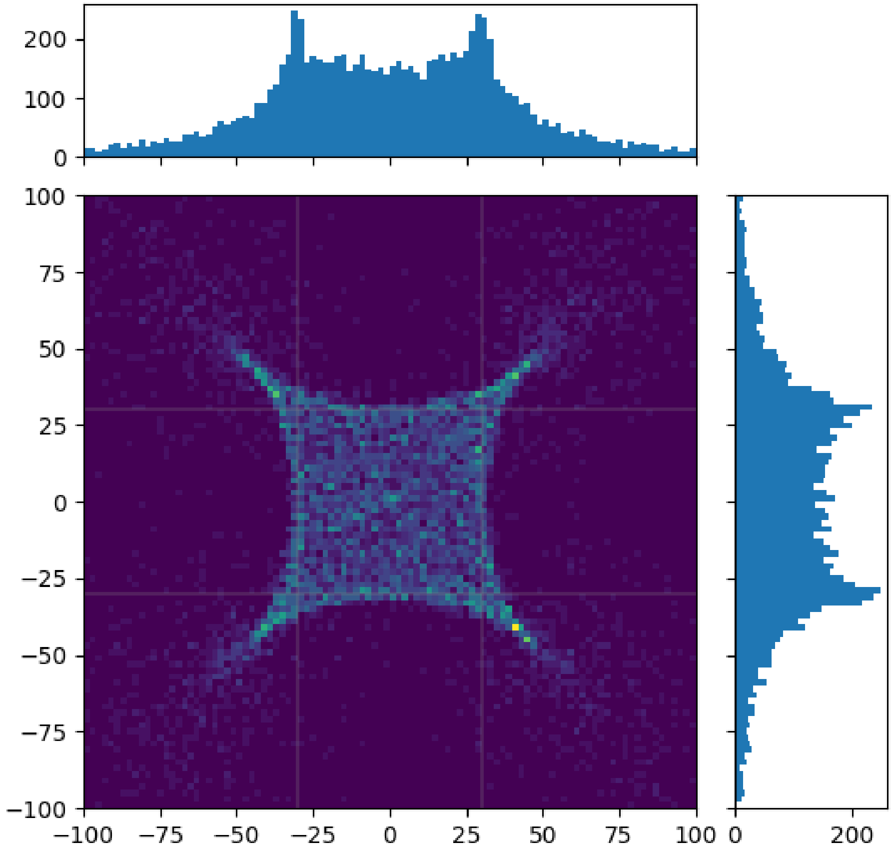

Lattice

Octupole Tracking – Comparison with Gaussian Bunch

How does this compare to the case with no octupole? What are the real-term gains?

- Uniform , Fewer Losses

SUCCESS

Clearly an improvement in uniformity in the region of interest. Tests used k-value = 30,000 mm^{-4}. Can be scaled up with more current to shape the beam further.

μ = 1.73

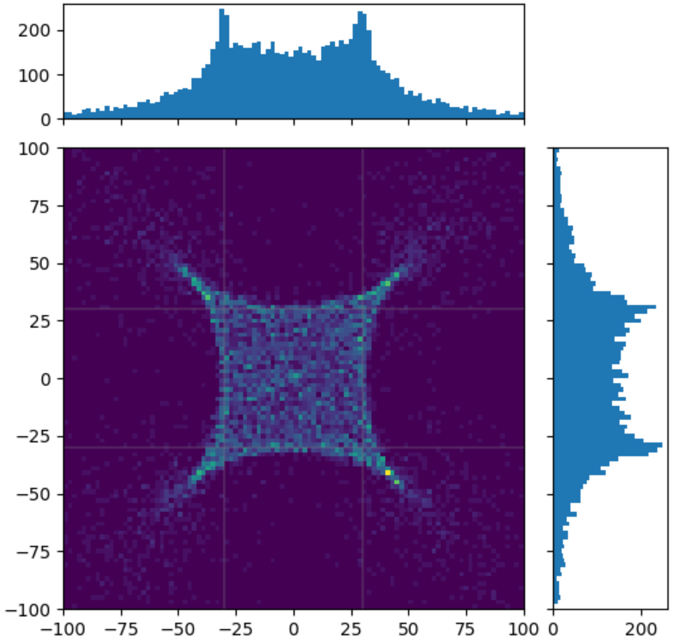

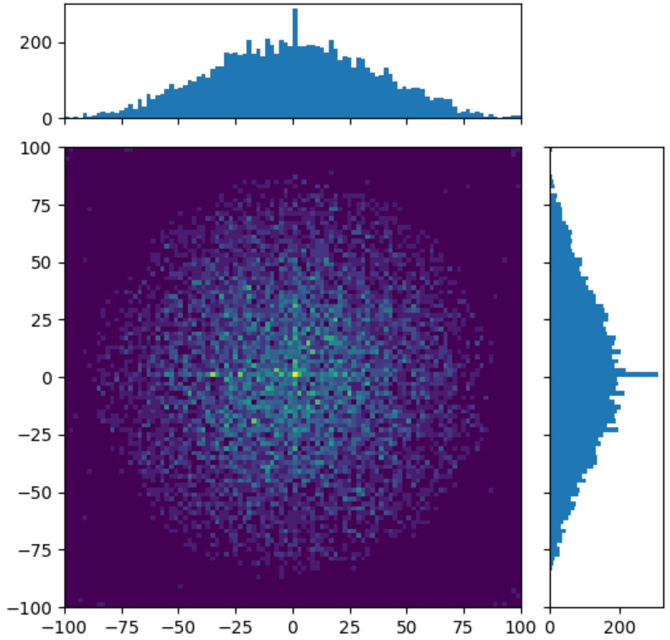

μ = 45.6

Lattice

Octupole: Capturing Missing Trends and Data

A single kurtosis measurement ignores many other features of the data like skewness ...

A quantile-quantile (QQ) plot directly compares the quantiles of two distributions to check for similarity. When one of those distributions is theoretical, we have what is known as a probability plot.

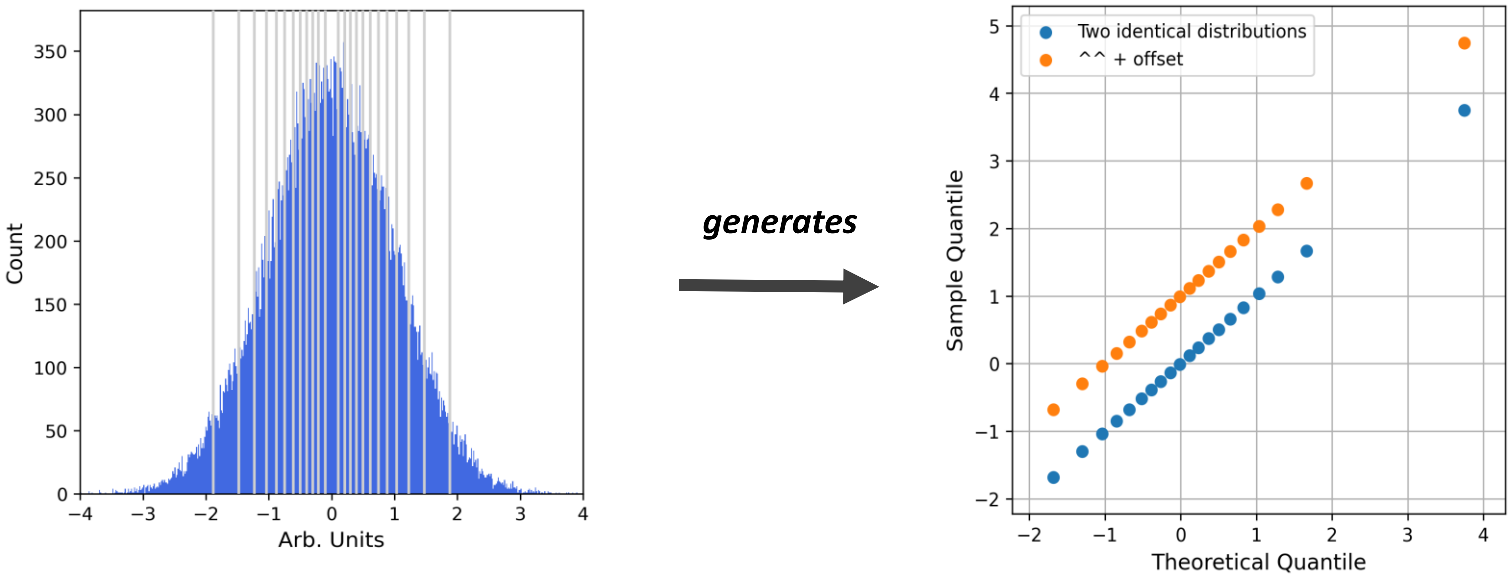

Octupole: Capturing Missing Trends and Data

Applying this to the octupole data …

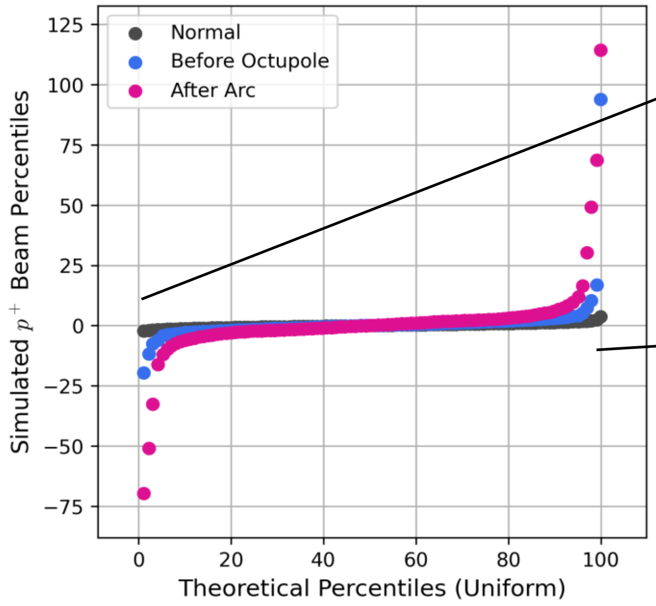

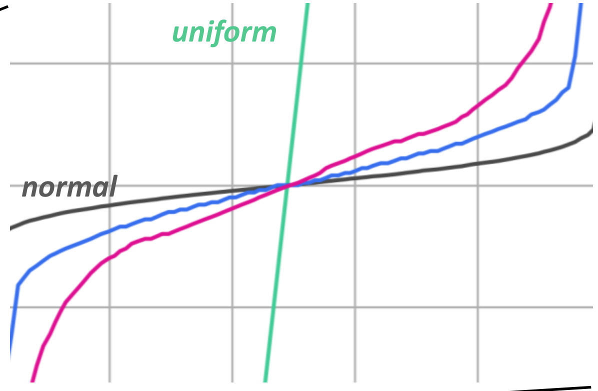

R1 = 0.60

R2 = 0.45

Outcome:

- Larger coefficient = better uniformity.
- Full distribution captured.
- Beam-beam comparisons possible.

Lattice

Gabor Lens Comparison

Performance study between solenoid and Gabor lens models in BDSIM

Confinement field neglected (~0.03T solenoid)

Plasma magnetic field negligible at proposed densities (~5e15 m^{-3})

Modelled as drift elements with field maps and scaling applied

Requires sufficient plasma density/uniformity to neutralise beam space charge and avoid instabilities

$$E_r = -\frac{e n_e r}{2\epsilon_0}$$

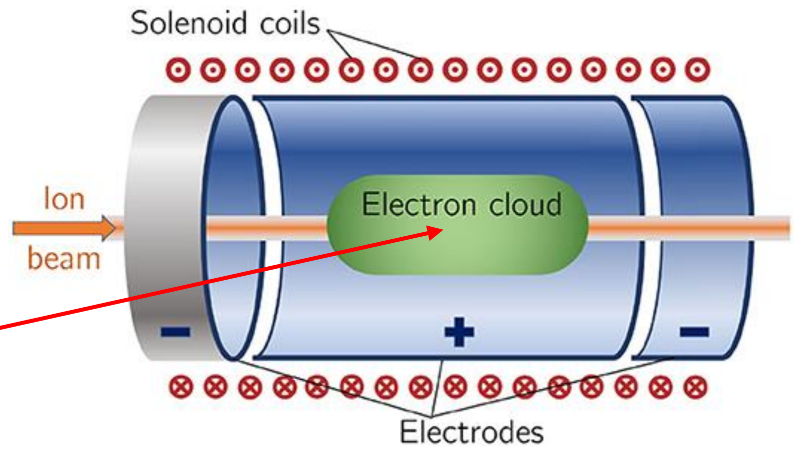

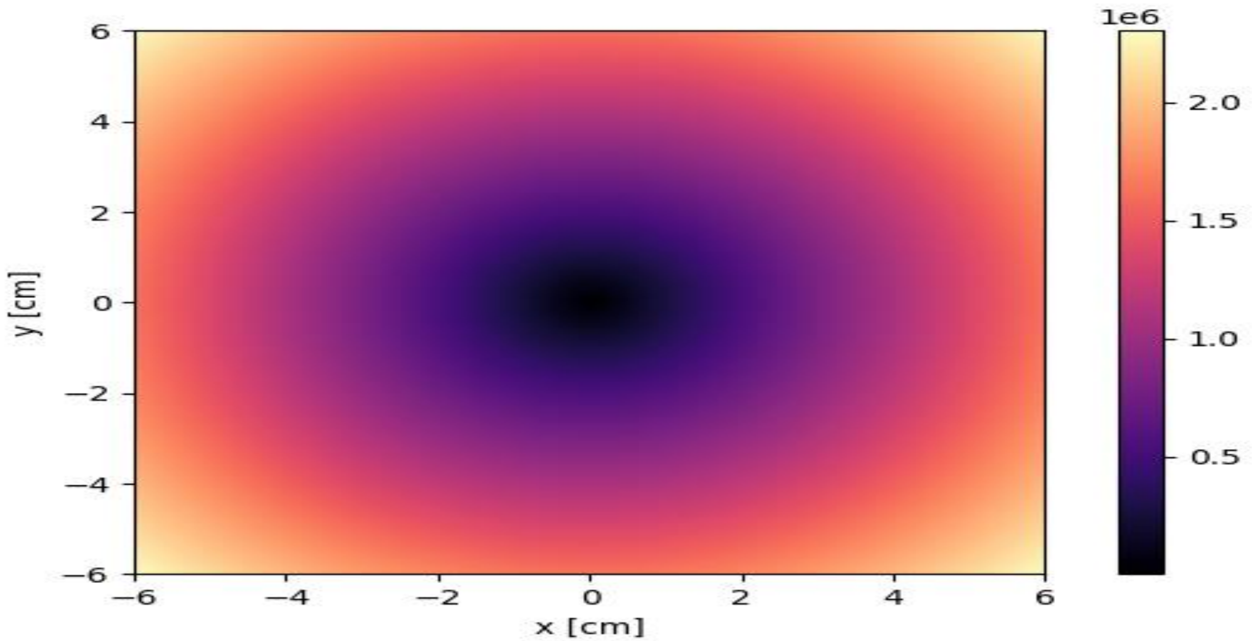

Field map equivalent to 1T

Gabor Lens Comparison

COBYLA optimisation for fine tuning optics [9]

Constraints remain satisfied

Solenoid strengths: 1.40, 0.57, 0.80, 1.04, 0.80, 1.40, 0.28

Gabor lens strengths: 1.38, 0.56, 0.81, 1.04, 0.80, 1.38, 0.32

Comparable strengths, same optics but much less power required

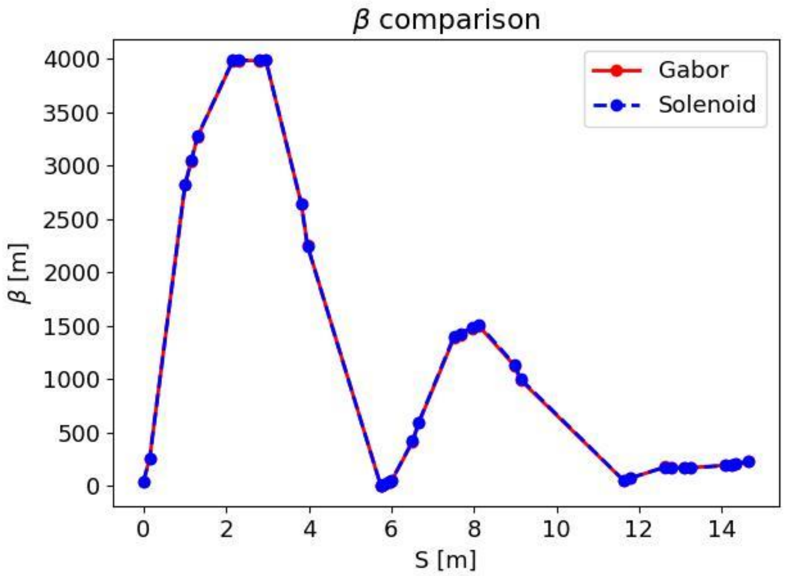

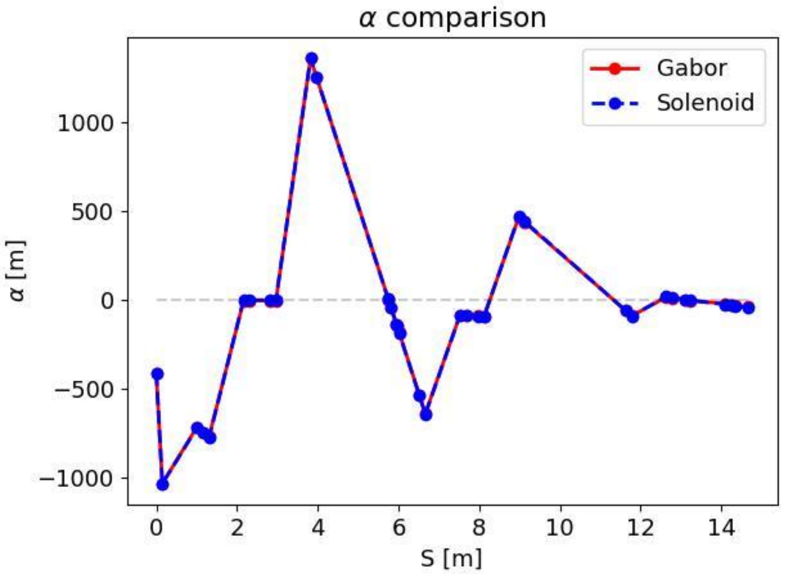

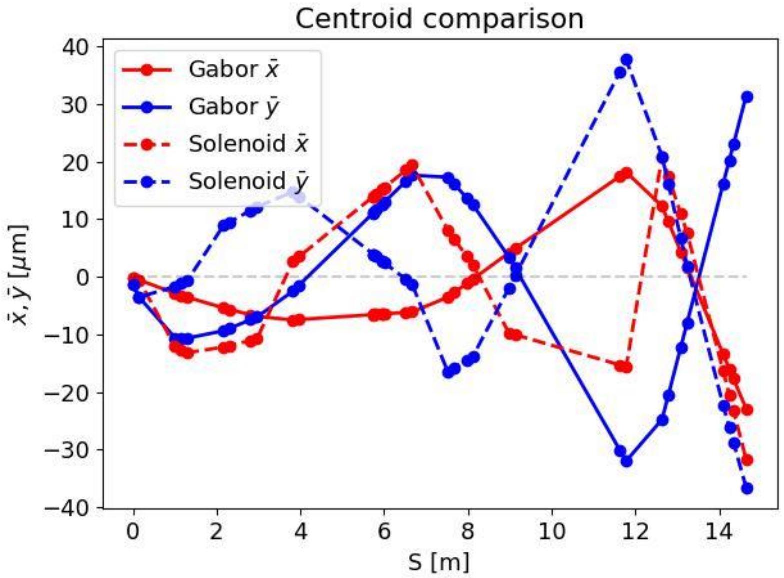

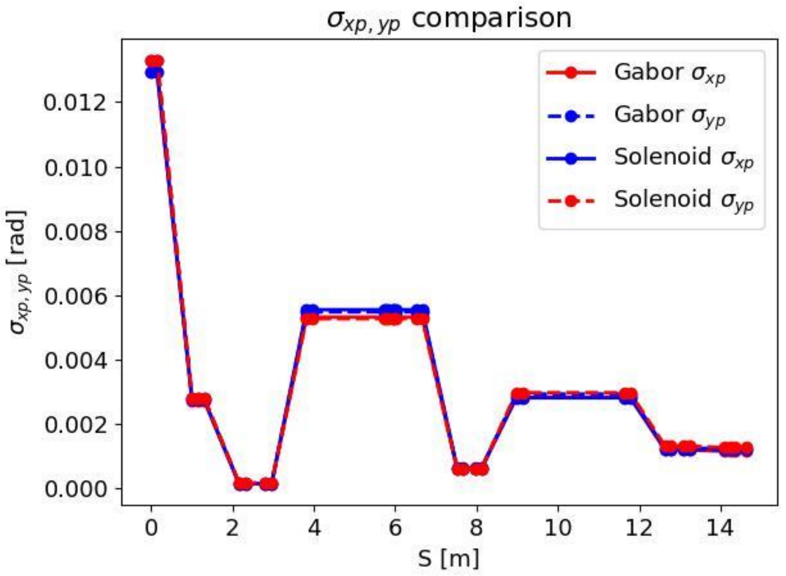

Lattice

RF Cavity Design

Giusy Passarelli (giusy.passarelli.2024@live.rhul.ac.uk)
Royal Holloway, University of London
Corey Lehmann (corey.lehmann@physics.ox.ac.uk)
University of Oxford
Carl Jolly (carl.jolly@physics.ox.ac.uk)
University of Oxford

RF Introduction and Requirements

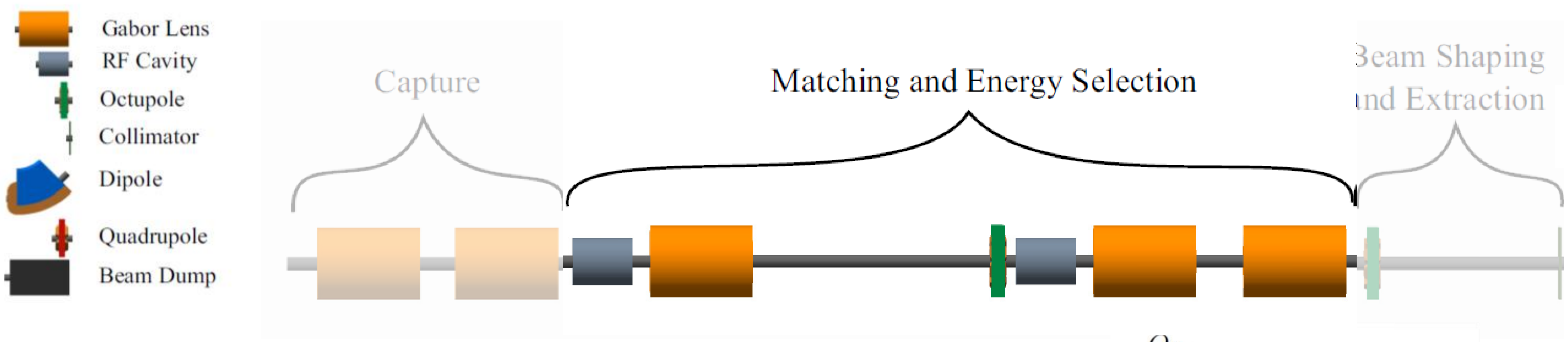

RF Cavity permits:

- Control of **bunch length;**
- Manipulation of the **longitudinal phase-space.**

$$V_{RF} = \frac{\Delta E^2 \pi h |\eta|}{2q\beta^2 E_s}$$

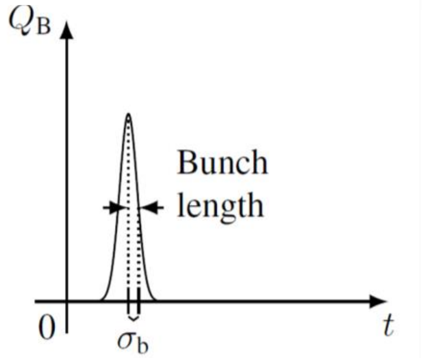

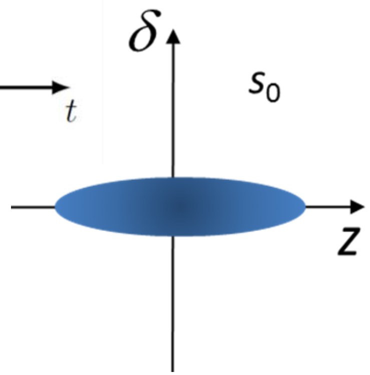

RF Cavity Requirements:

- Beam Energy = 15MeV
- Total relative energy spread = ± 2%
- Initial bunch length ~ 10 fs
- Distance between the beam source and the first RF Cavity ≅ 3m

Frequency Choice

- RF frequency tuned for bunch length alignment on rising RF wave edge.
- Late particles (closer to the bunch end) gain energy, while early ones (closer to the beginning) lose it, ensuring **phase stability**.
- All particles receive a positive acceleration at the same time, and the beam remains grouped throughout its trajectory.

Frequency	Bunch Length "Stability"
201 MHz	2.5 ns
352 MHz	1.4 ns

- Energy spread > 2% $\Rightarrow$ Frequency < 201MHz

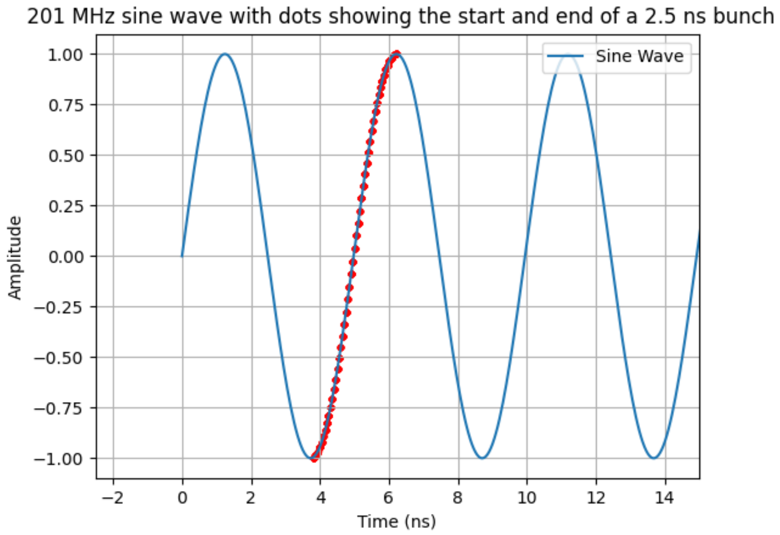

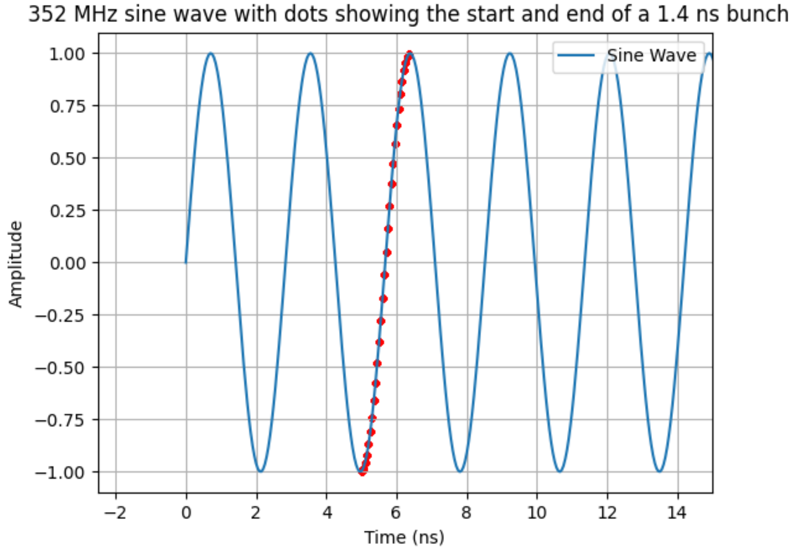

SuperFish CCL Geometry

8 Free Parameters:
- **Length**
- **Gap Length**
- Outer Corner Radius
- Inner Corner Radius
- Outer Nose Radius
- Inner Nose Radius
- Flat Length
- Cone Angle

Automatically adjusts diameter to fit frequency

Automatically adjusts E field to reach Kilpatrick factor of 1.5

Optimising for:
- Shunt Impedance
- Transit Time
- **Bunching Capability**

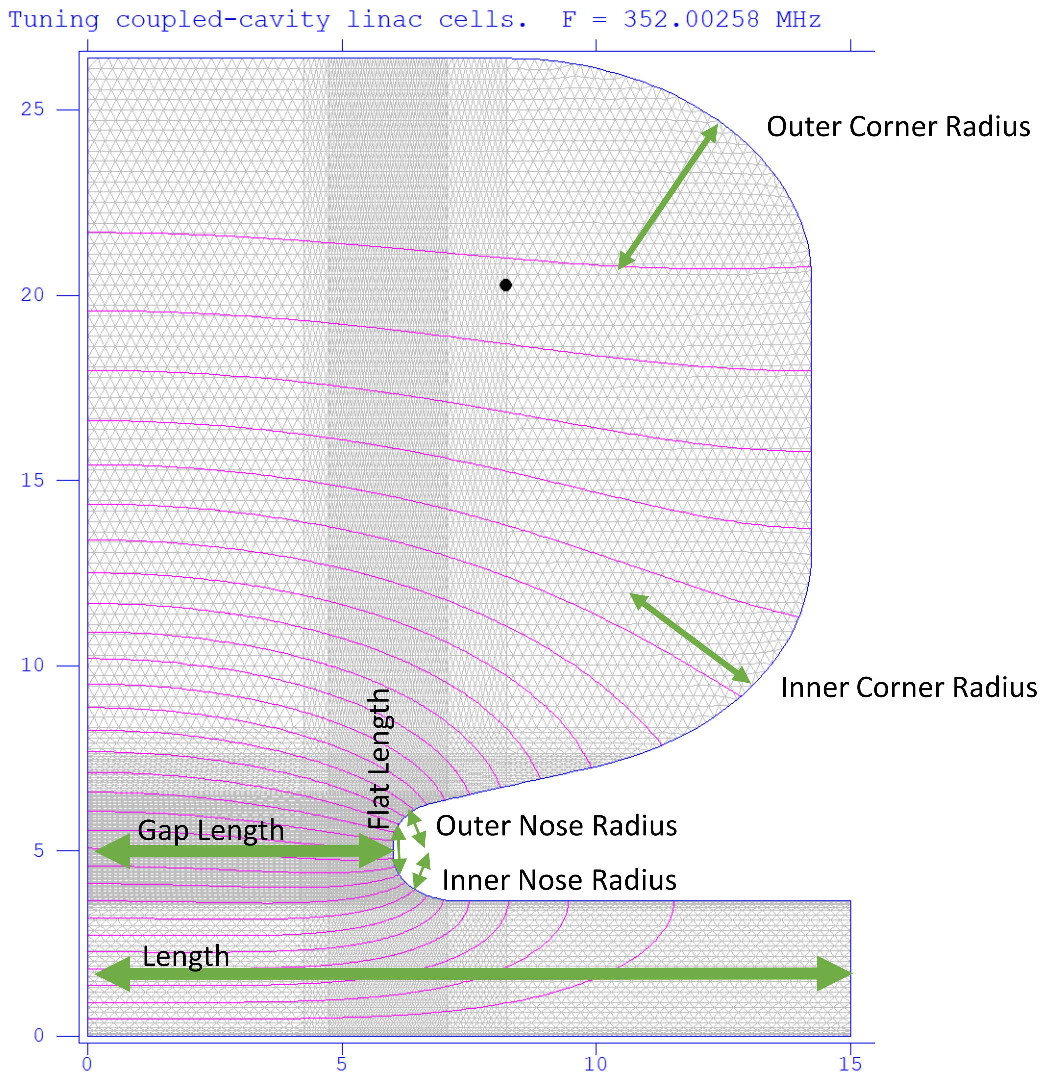

Cavity Optimisation

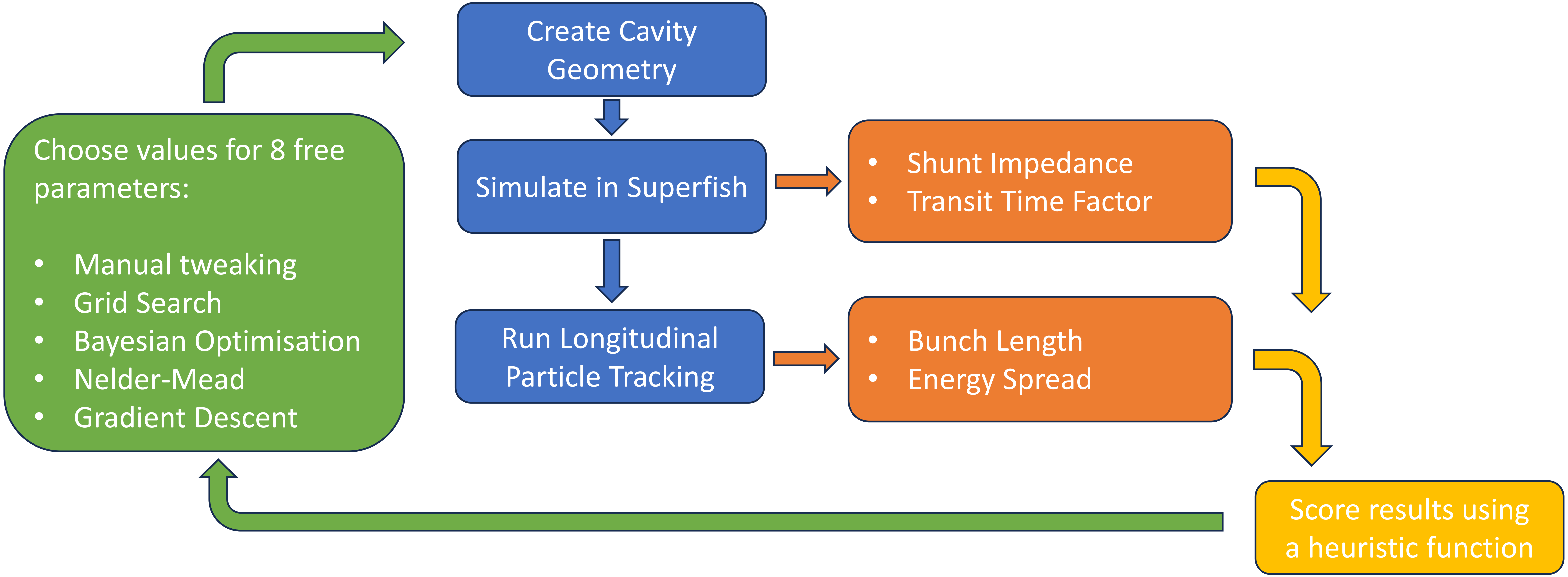

Longitudinal Particle Tracking

Need a way to measure bunching ability for each cavity design.

- Write a simple particle-tracking simulation code
- Generate N particles representing bunch distribution
- Treat most of accelerator as drift
- On passing through the RF cavity, change the energy of the particle based on the field profile calculated in SuperFish
- Record the bunch length and energy spread at exit

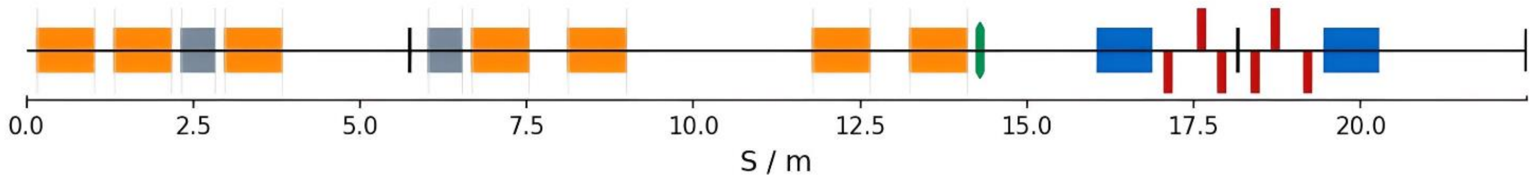

Longitudinal Phase Space Simulation – Cavities OFF

Energy: 15 ± 0.29 MeV (1.92%)
Bunch Length: 0.82 ns

15 MeV Protons

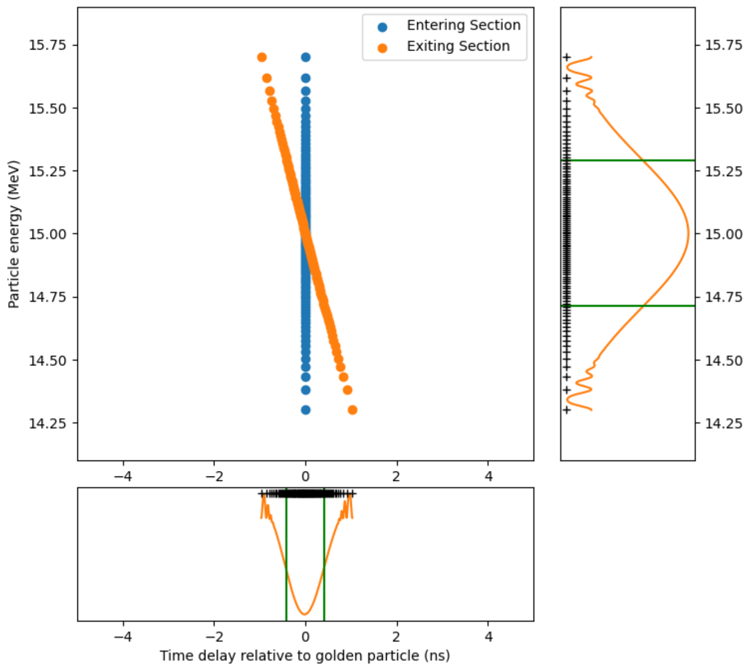

4 MeV/u Carbons

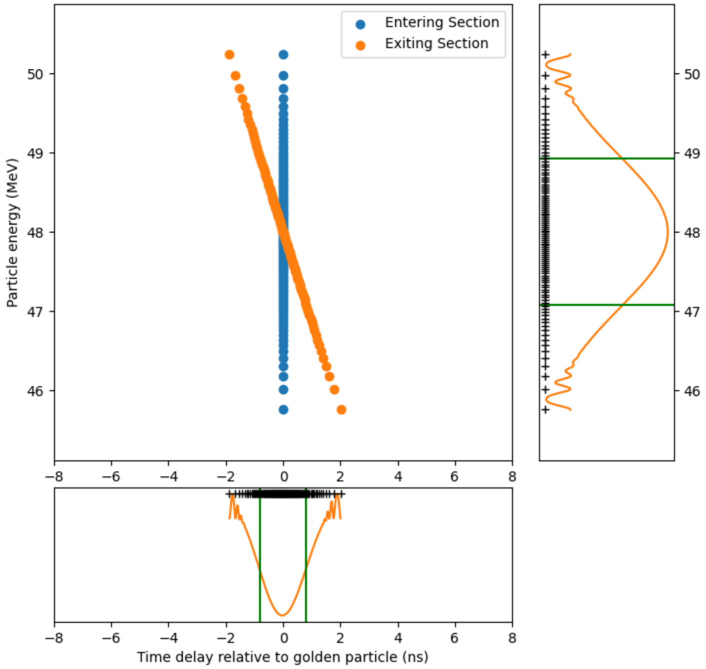

Energy: 48 ± 0.92 MeV (1.92%)
Bunch Length: 1.60 ns

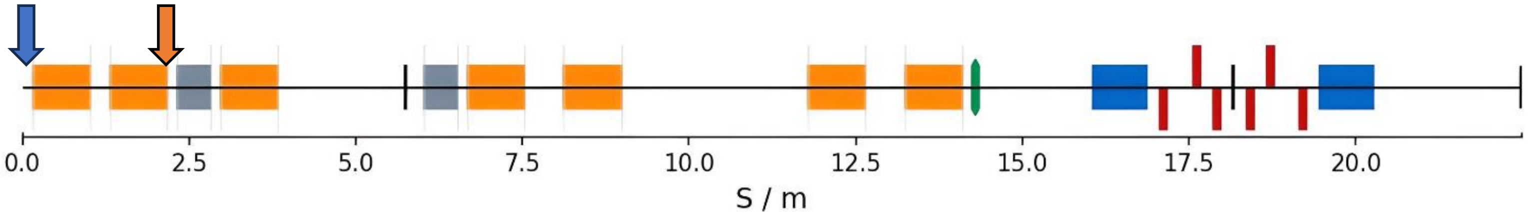

RF Cavities

Longitudinal Phase Space Simulation – Cavities OFF

15 MeV Protons

Energy: 15 ± 0.29 MeV (1.92%)
Bunch Length: 1.00 ns

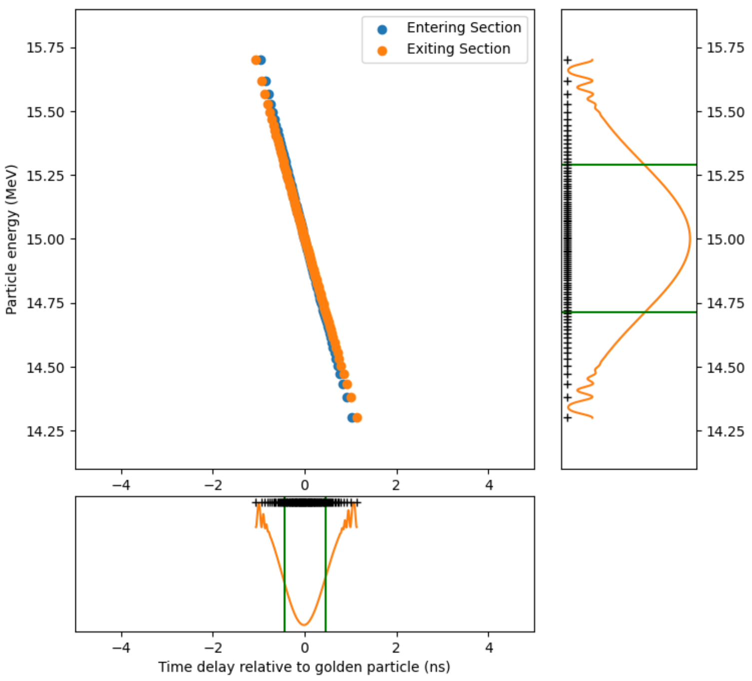

4 MeV/u Carbons

Energy: 48 ± 0.92 MeV (1.92%)
Bunch Length: 1.94 ns

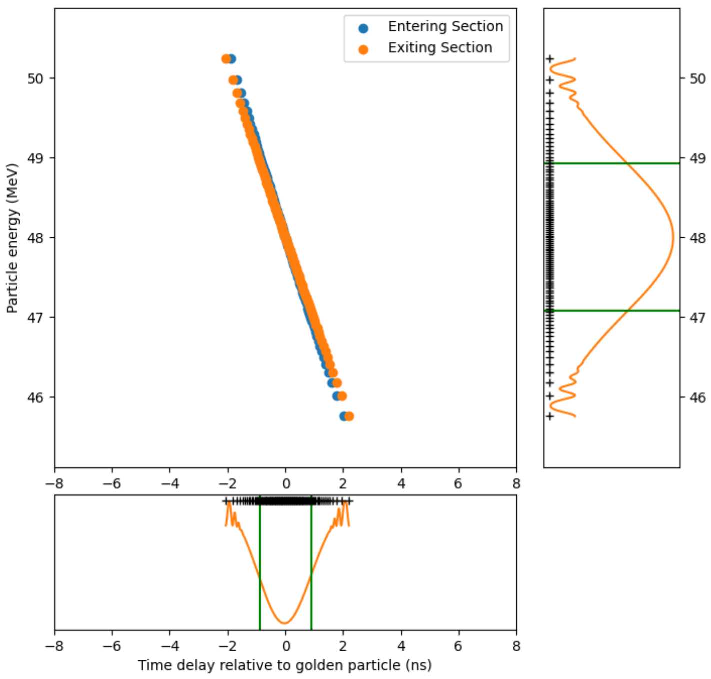

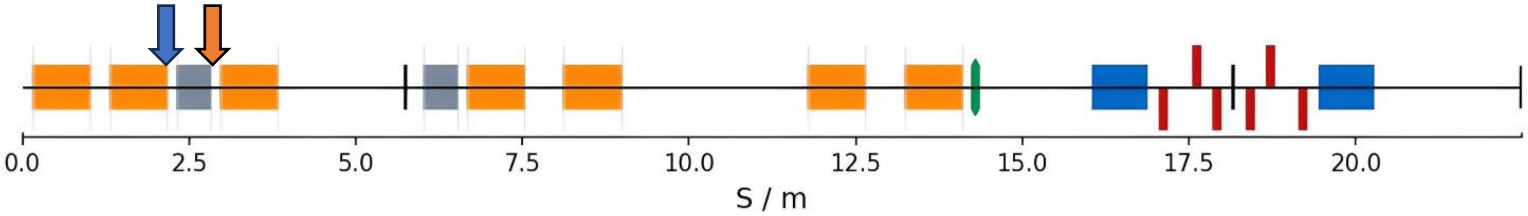

RF Cavities

Longitudinal Phase Space Simulation – Cavities OFF

15 MeV Protons

Energy: 15 ± 0.29 MeV (1.92%)
Bunch Length: 2.14 ns

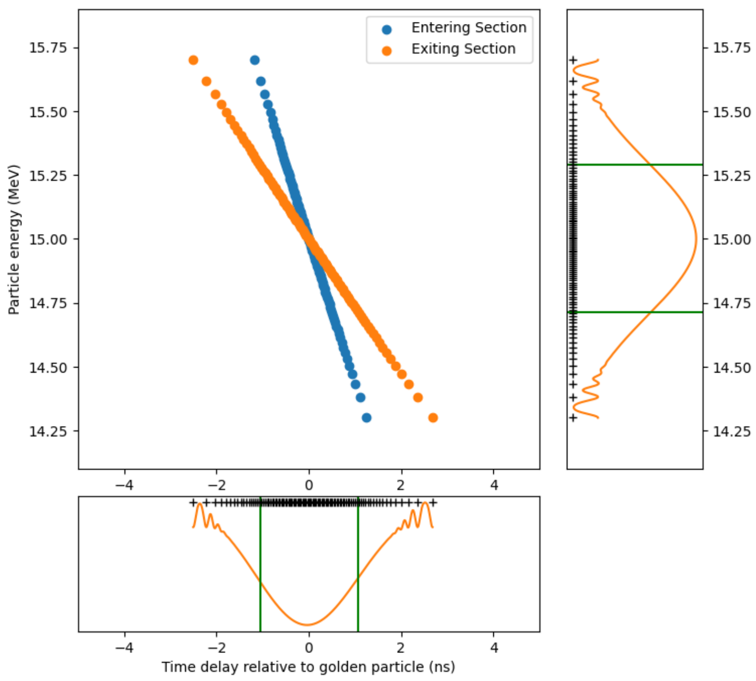

4 MeV/u Carbons

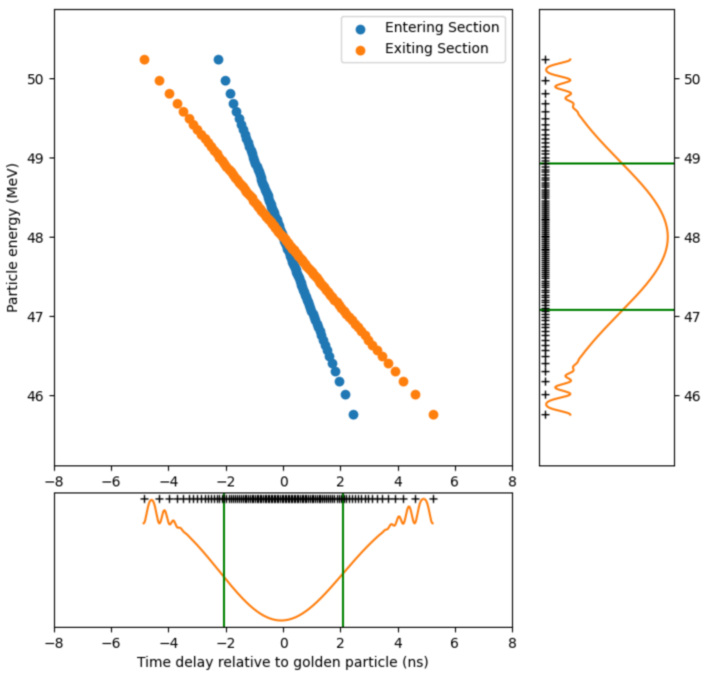

Energy: 48 ± 0.92 MeV (1.92%)
Bunch Length: 4.16 ns

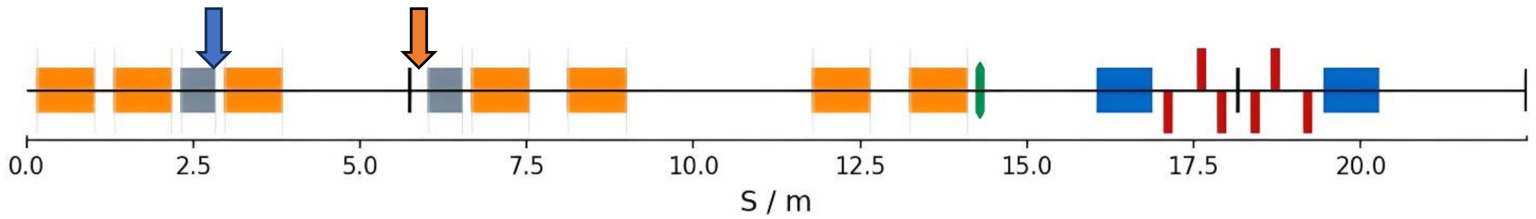

RF Cavities

Longitudinal Phase Space Simulation – Cavities OFF

Energy: 15 ± 0.29 MeV (1.92%)
Bunch Length: 2.32 ns

15 MeV Protons

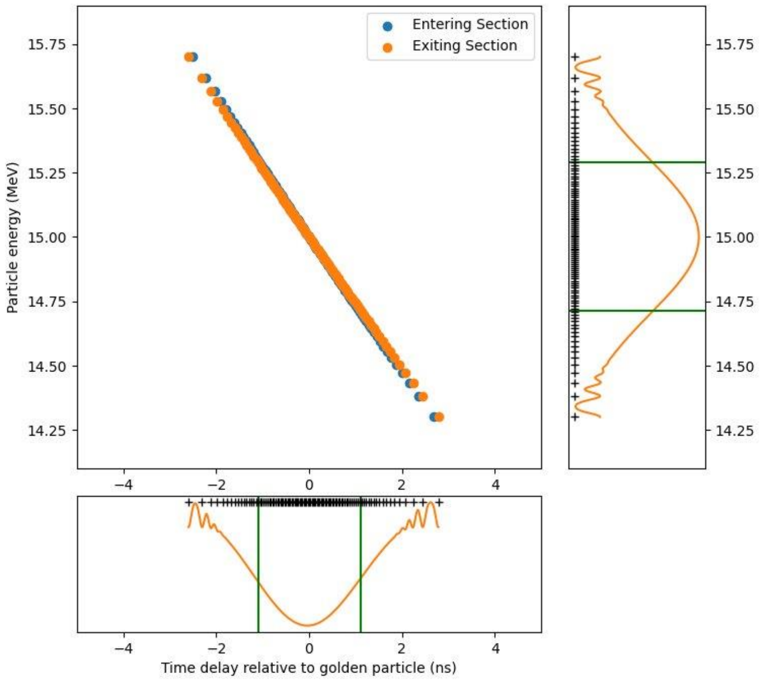

4 MeV/u Carbons

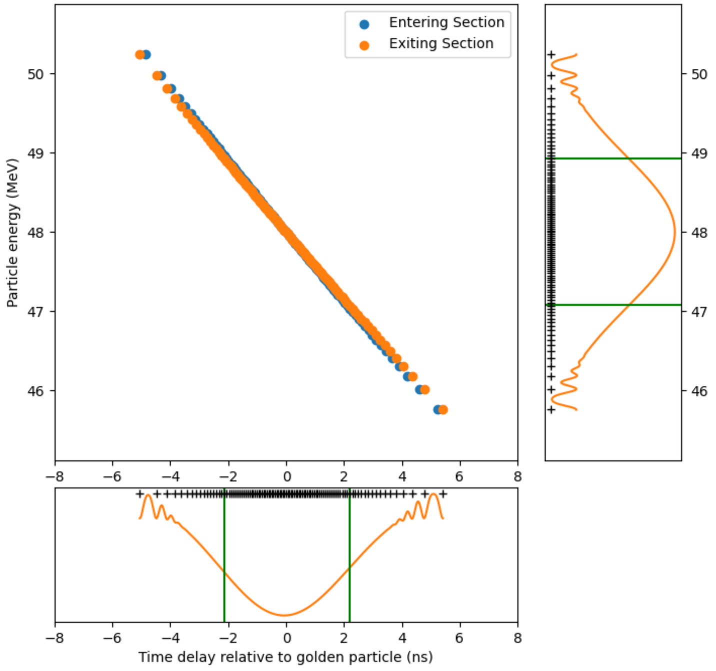

Energy: 48 ± 0.92 MeV (1.92%)
Bunch Length: 4.50 ns

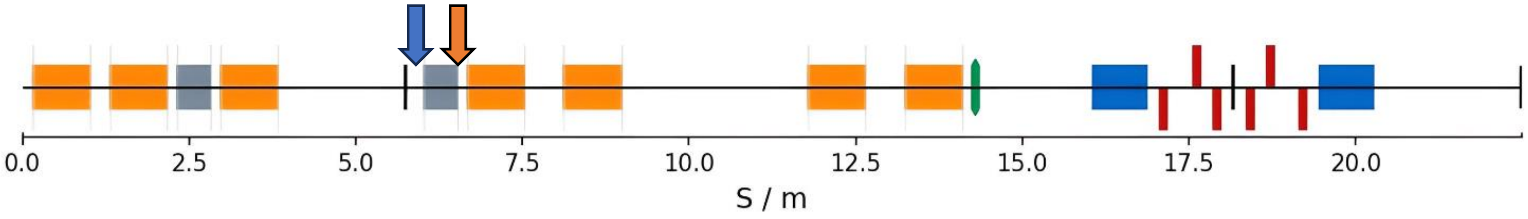

RF Cavities

Longitudinal Phase Space Simulation – Cavities OFF

Energy: 15 ± 0.29 MeV (1.92%)
Bunch Length: 4.00 ns

15 MeV Protons

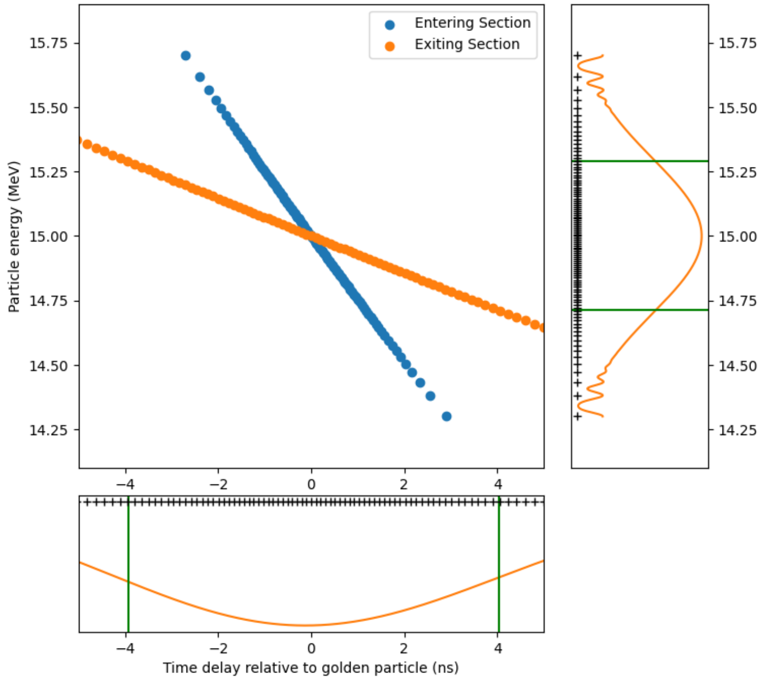

4 MeV/u Carbons

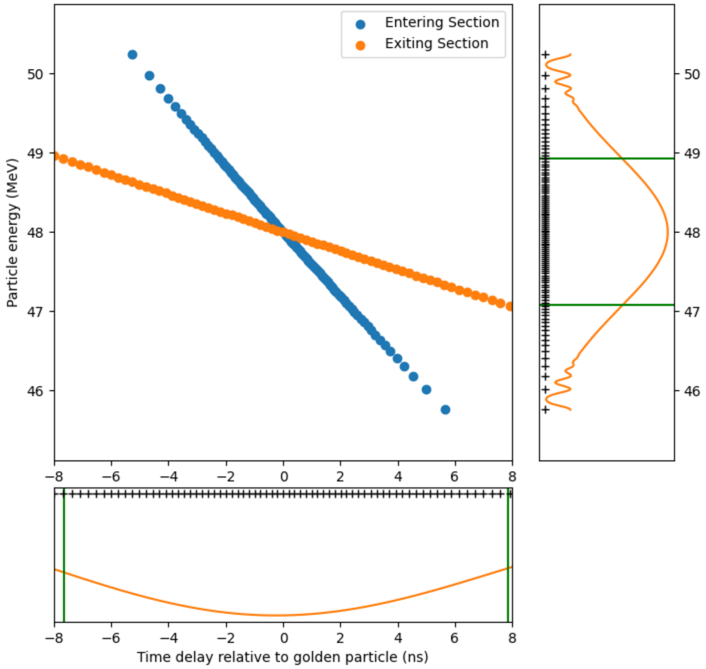

Energy: 48 ± 0.92 MeV (1.92%)
Bunch Length: 15.50 ns

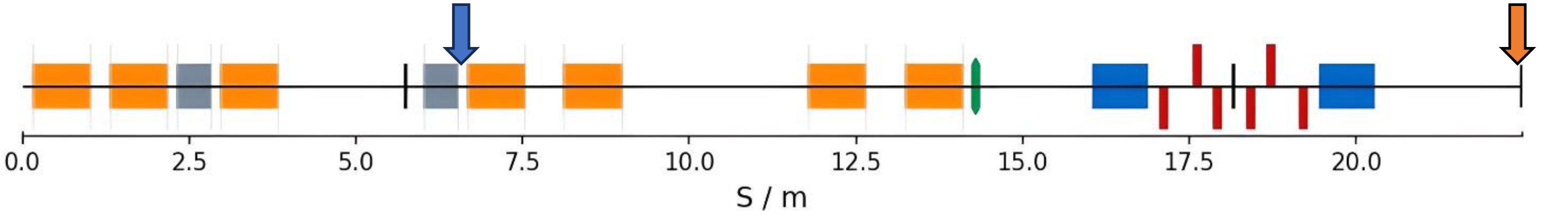

RF Cavities

Longitudinal Phase Space Simulation – Cavities ON

15 MeV Protons

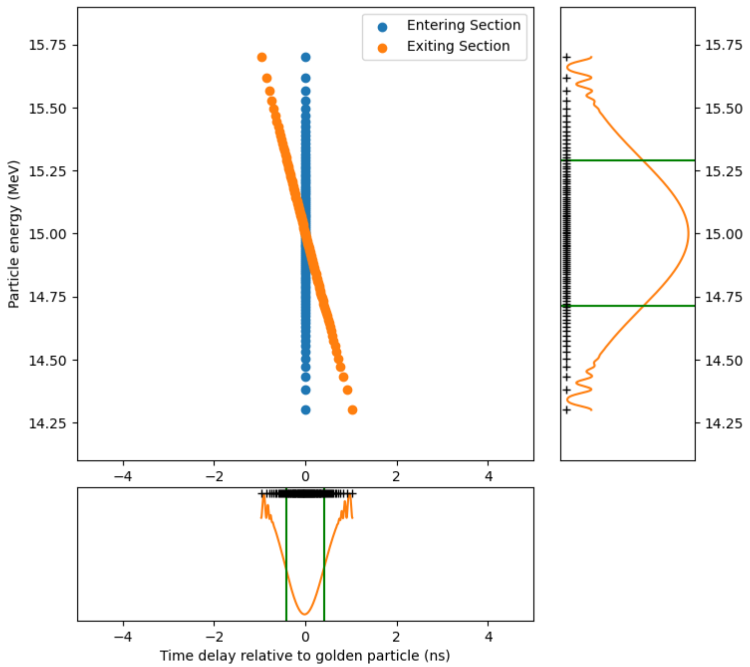

Energy: 15 ± 0.29 MeV (1.92%)
Bunch Length: 0.82 ns

4 MeV/u Carbons

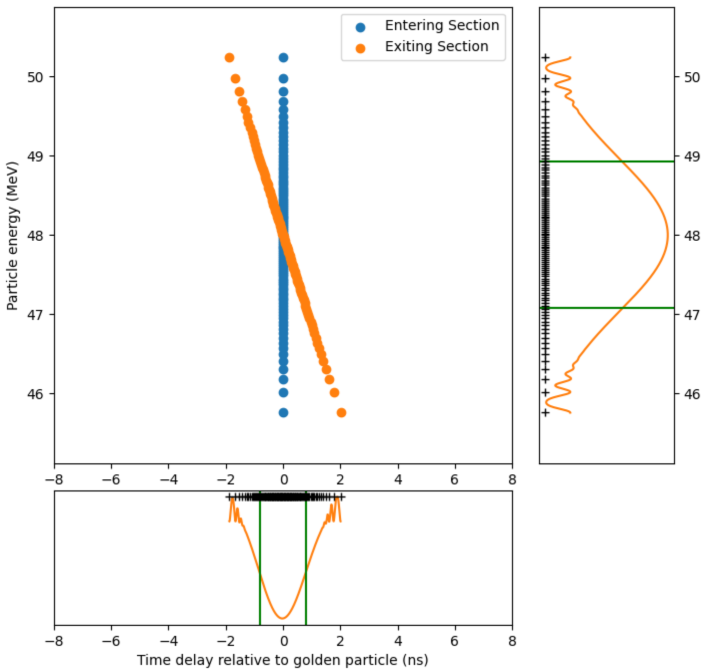

Energy: 48 ± 0.92 MeV (1.92%)
Bunch Length: 1.60 ns

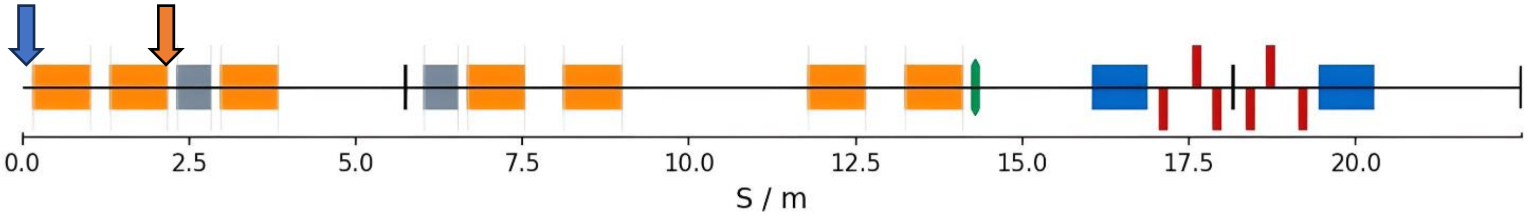

RF Cavities

Longitudinal Phase Space Simulation – Cavities ON

15 MeV Protons

Energy: 15 ± 0.09 MeV (0.61%)
Bunch Length: 0.90 ns

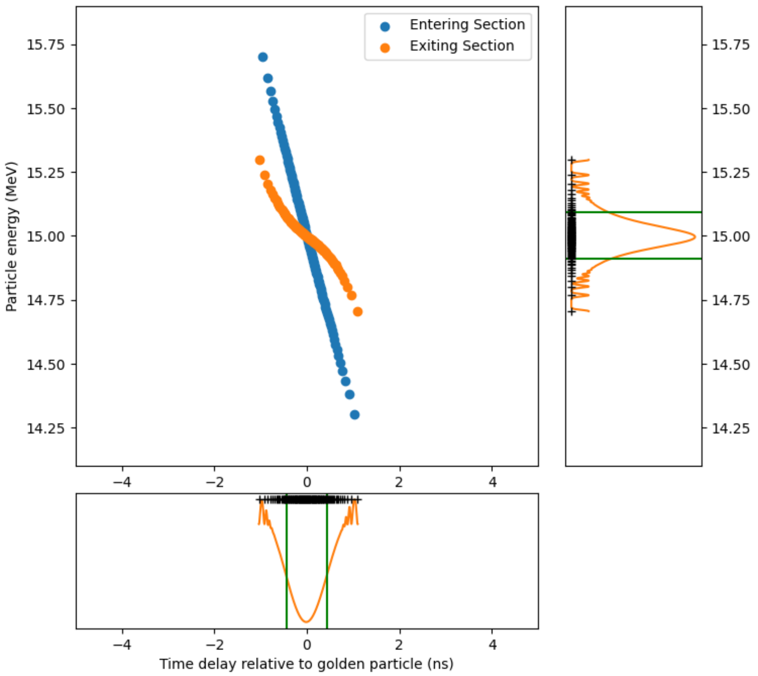

4 MeV/u Carbons

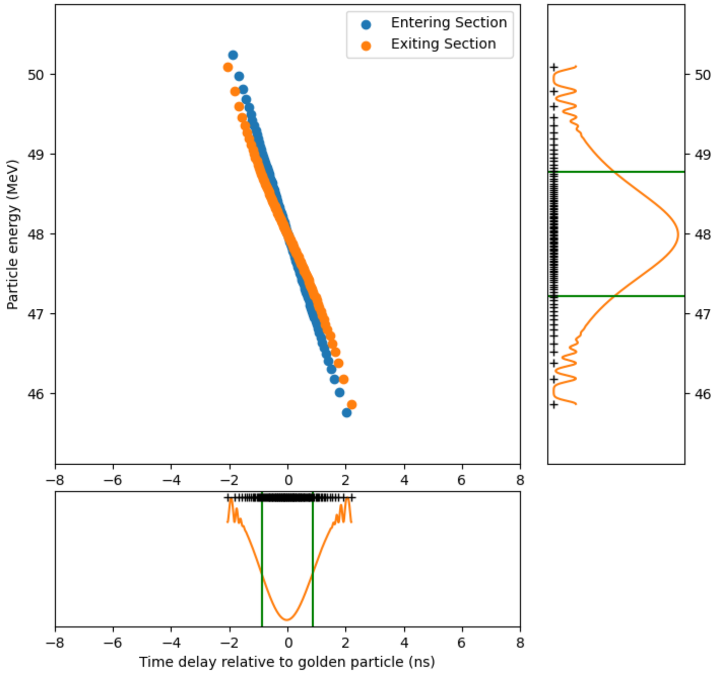

Energy: 48 ± 0.78 MeV (1.62%)
Bunch Length: 1.90 ns

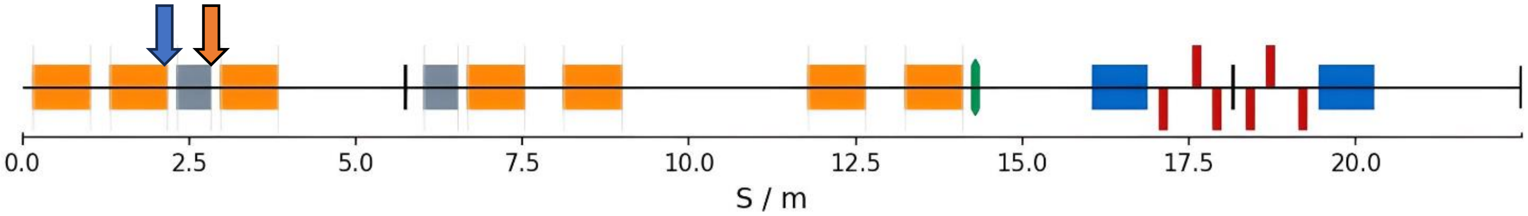

RF Cavities

Longitudinal Phase Space Simulation – Cavities ON

15 MeV Protons

Energy: 15 ± 0.09 MeV (0.61%)
Bunch Length: 1.26 ns

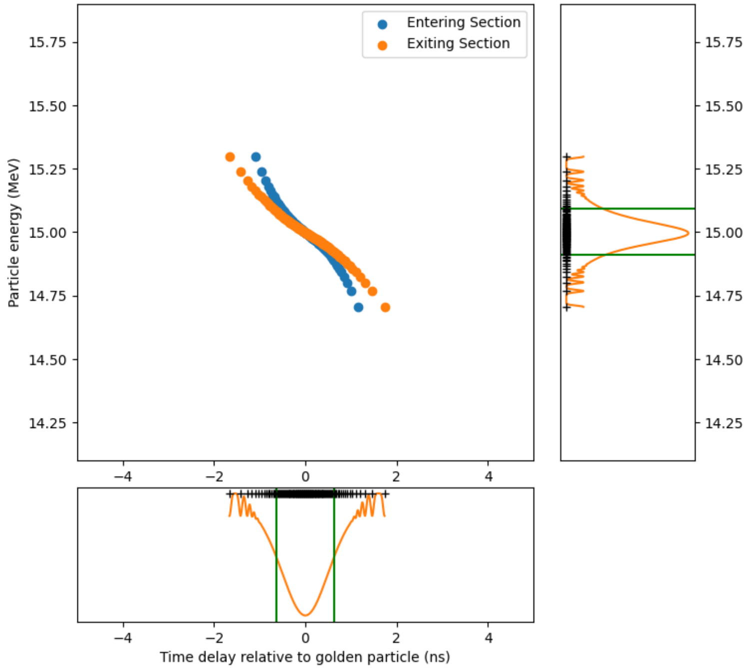

4 MeV/u Carbons

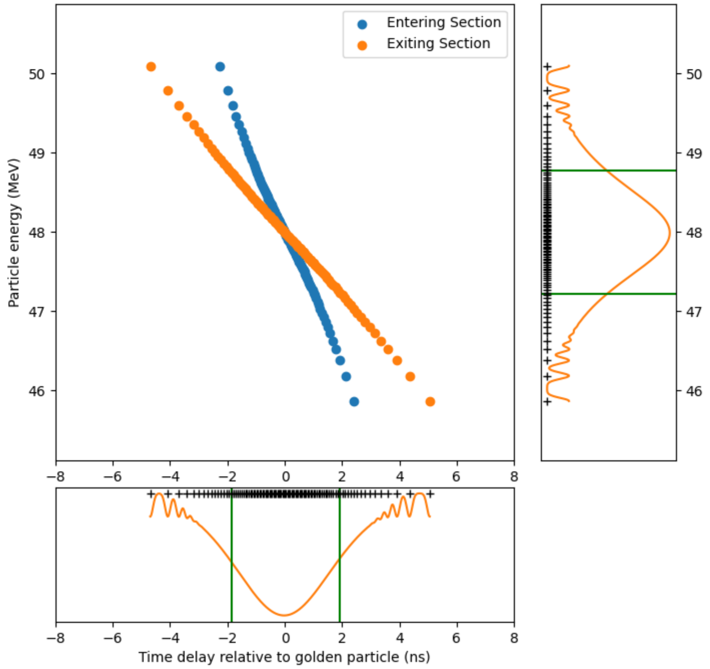

Energy: 48 ± 0.92 MeV (1.62%)
Bunch Length: 3.76 ns

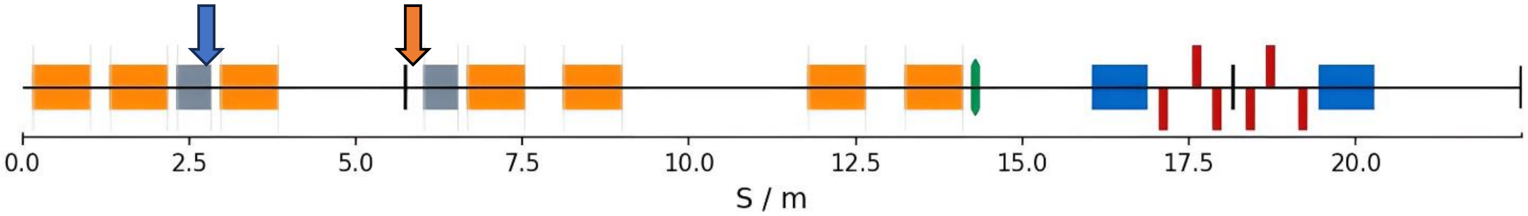

RF Cavities

Longitudinal Phase Space Simulation – Cavities ON

Energy: 15 ± 0.05 MeV (0.31%)
Bunch Length: 1.26 ns

Operating at 45% of Design E-field

15 MeV Protons

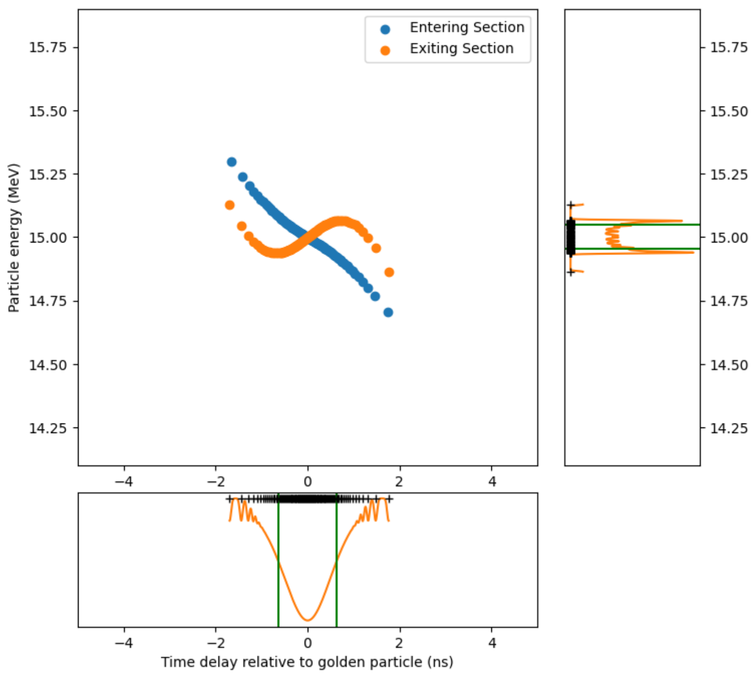

4 MeV/u Carbons

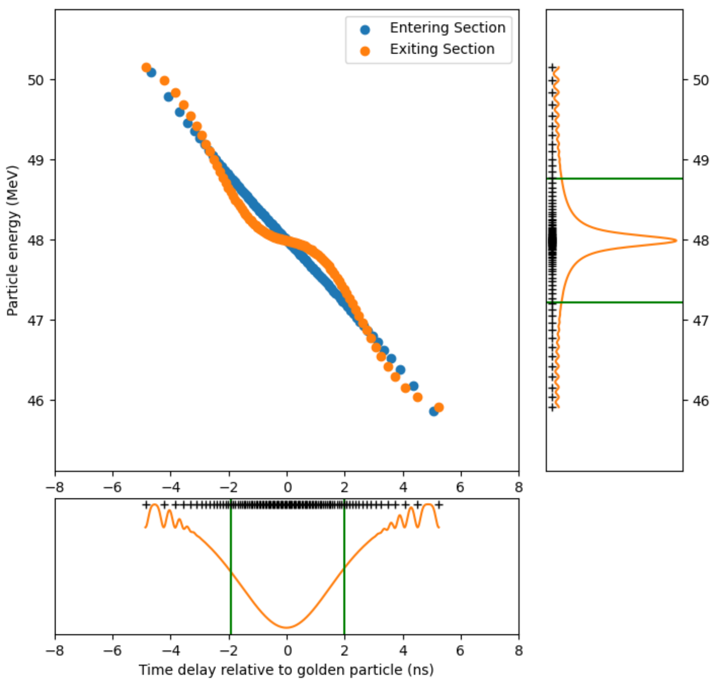

Energy: 48 ± 0.77 MeV (1.61%)
Bunch Length: 4.04 ns

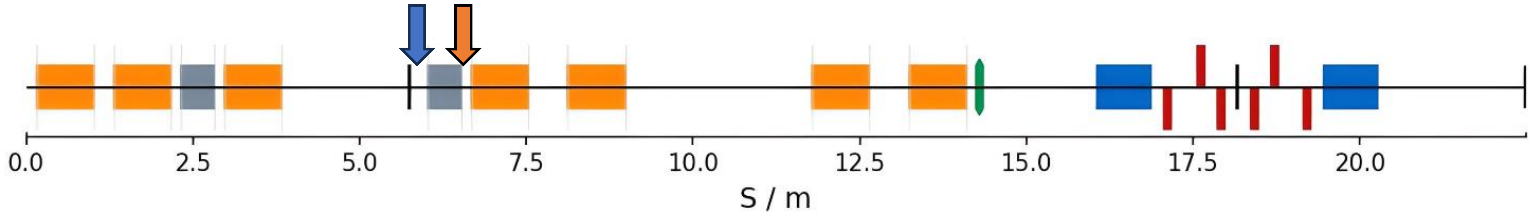

RF Cavities

Longitudinal Phase Space Simulation – Cavities ON

15 MeV Protons

Energy: 15 ± 0.05 MeV (0.31%)
Bunch Length: 1.18 ns

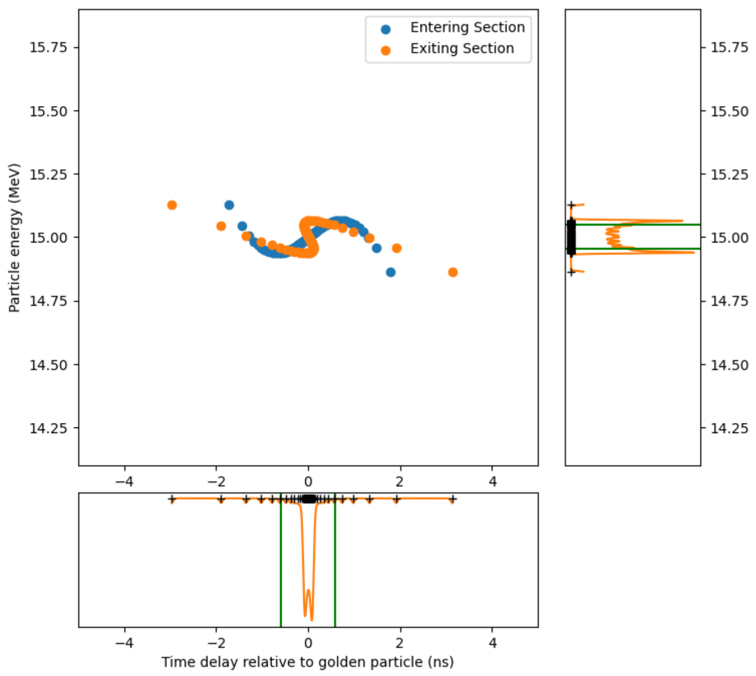

4 MeV/u Carbons

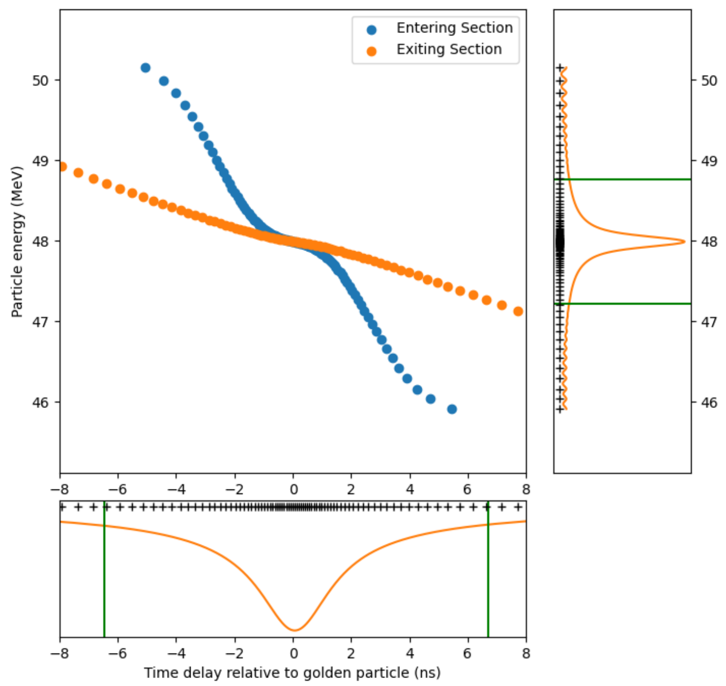

Energy: 48 ± 0.77 MeV (1.61%
Bunch Length: 13.16 ns

Highly non-gaussian bunch
shapes not described well b
standard deviation metric

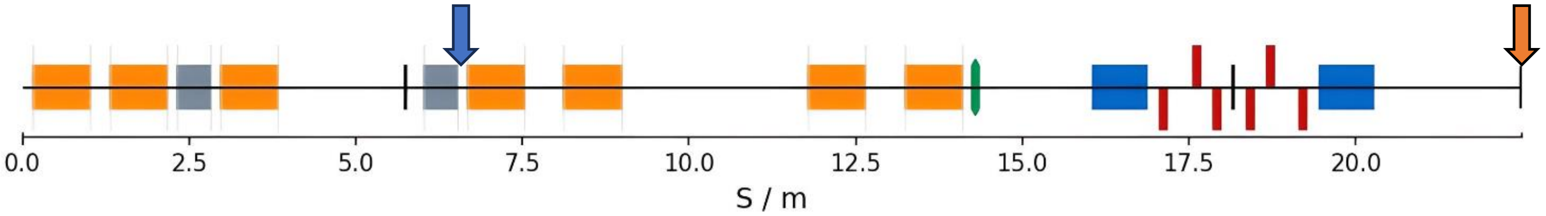

RF Cavities

Longitudinal Phase Space Simulation – Results

15 MeV Protons

OFF

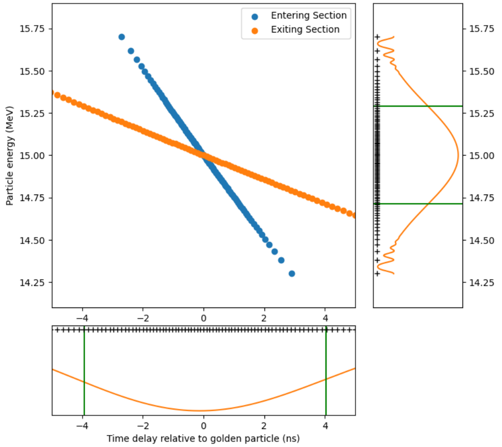

ON

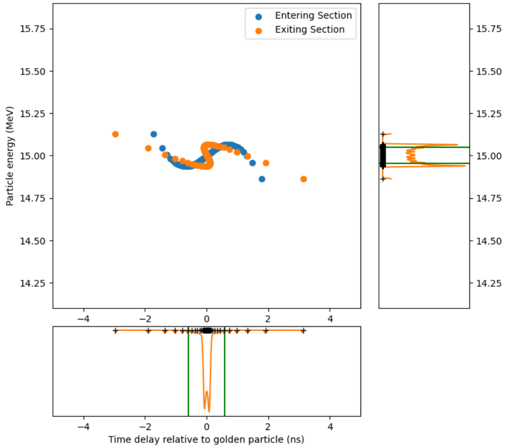

Bunch Length	Energy Spread
4.00 ns	1.92%
1.18 ns	0.31%

4 MeV/u Carbons

OFF

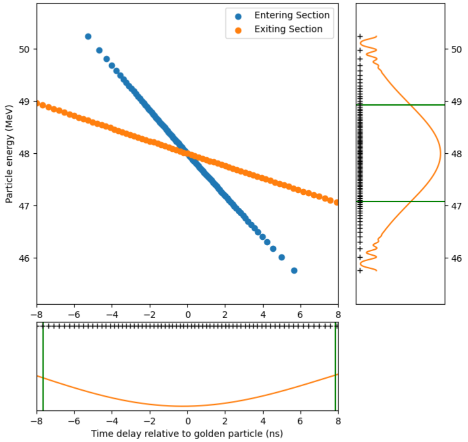

ON

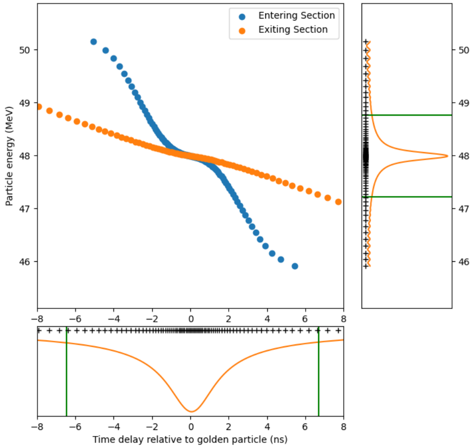

Bunch Length	Energy Spread
15.50 ns	1.92%
13.16 ns	1.61%

RF Cavities

Final Cavity Geometry

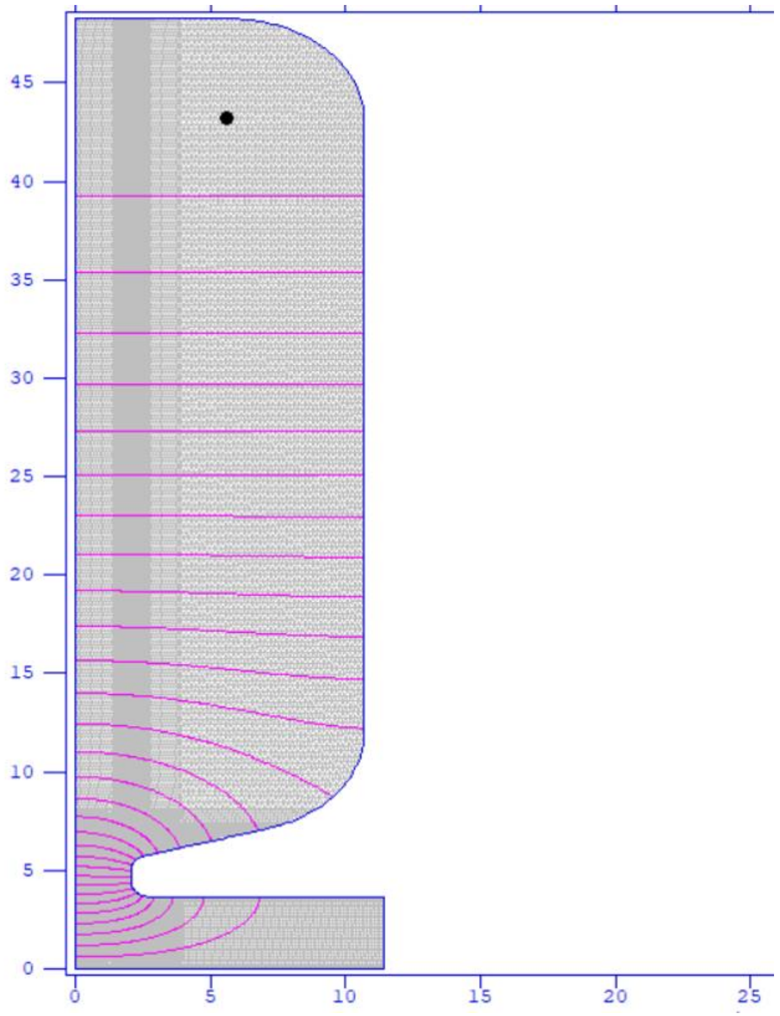

Parameter	Value
Frequency [MHz]	201
Shunt Impedance - Z [MOhm/m]	25.41
Transit time factor -T []	0.33
ZTT [MOhm/m]	2.91
Maximum E field [MV/m] @ kilpatrick – 1.5	22.15
Maximum E field on axis [MV/m] @ kilpatrick – 1.5	8.08

3D Simulation with CST

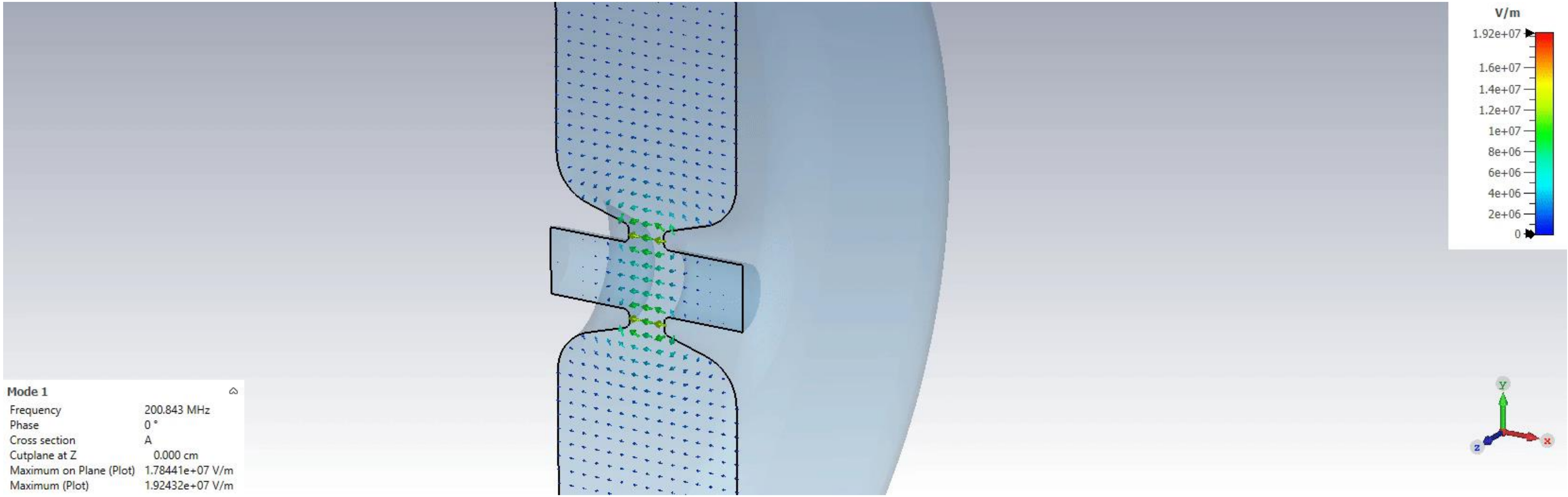

SuperFish vs CST

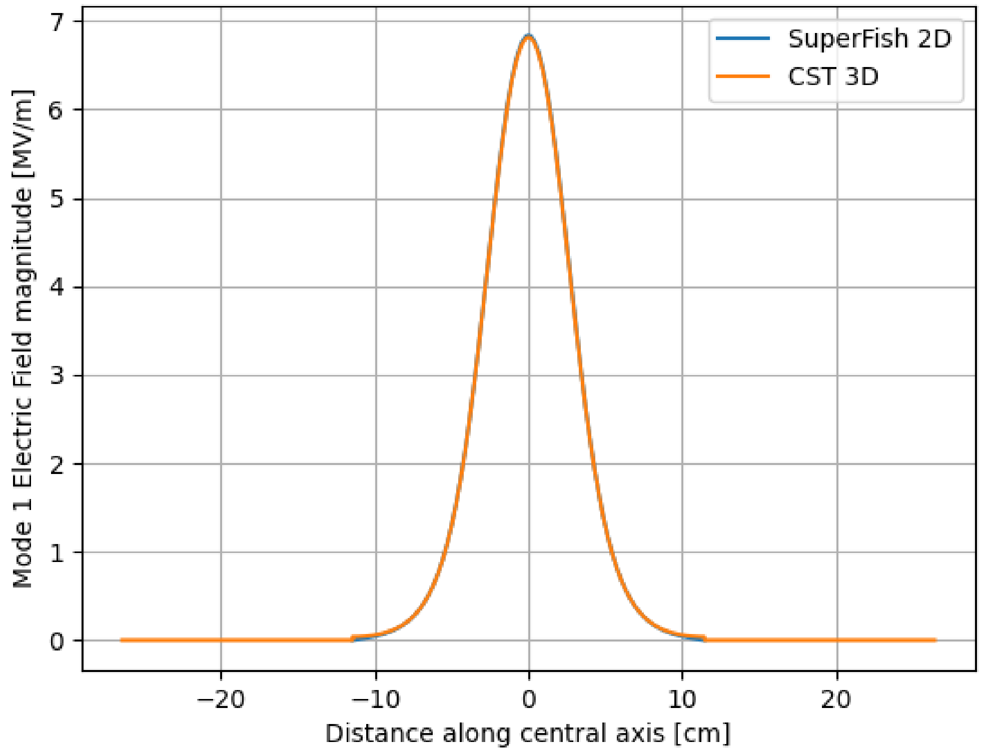

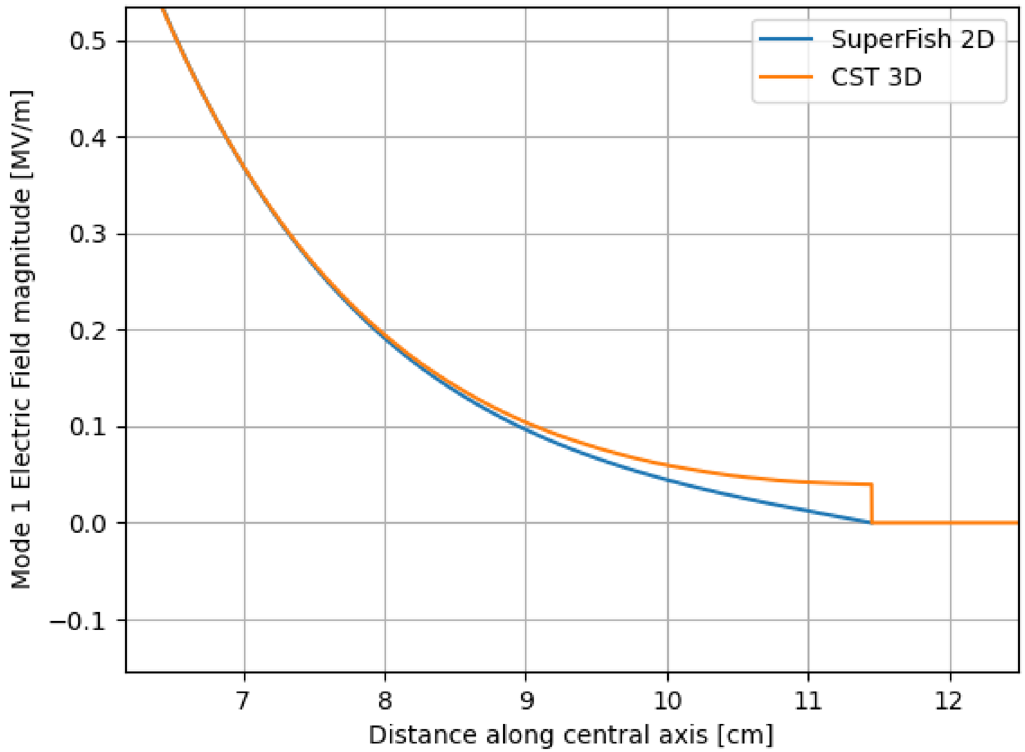

- Scaled by the stored energy in the cavity.
- Size of the electric field is somewhat arbitrary. We are looking a relative differences here.

Simulation of the 3D Field Map in the BDSIM Lattice

- Simulation in BDSIM using the 3D field map from CST.
- Validated the cavity design and shown good control of the longitudinal phase space
- Final energy spread 0.68%

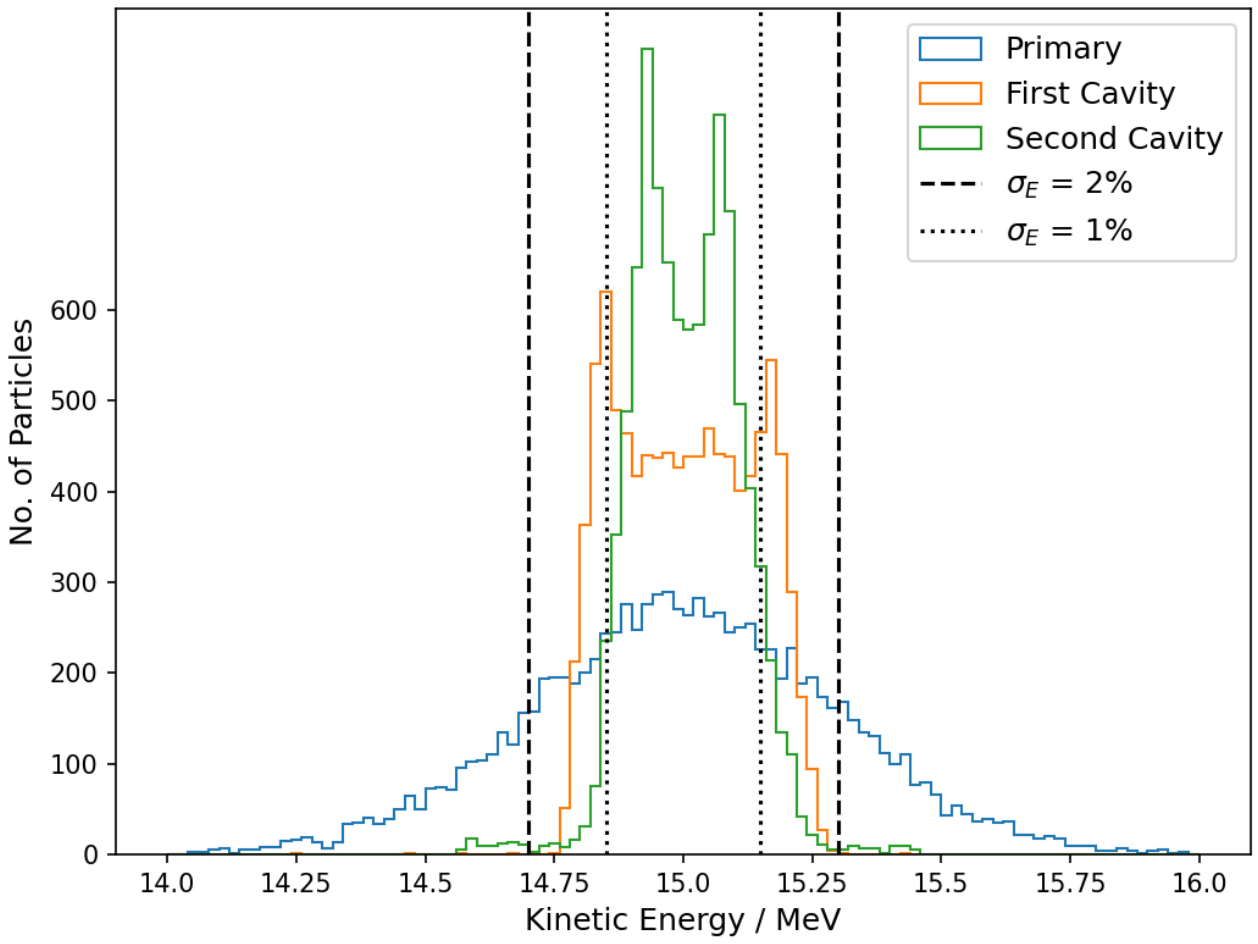

RF Cavities

RF Cavities Summary

- Designed & optimised a 3D cavity design for LhARA stage 1.
- Validated the design with 6D tracking in BDSIM.

Future work:

- Investigate schemes to better control the carbon beam.
- Continue design is CST, waveguides and waveguide ports.
- Continue optimisation using BDSIM.
- Additional RF infrastructure, cavity phasing.

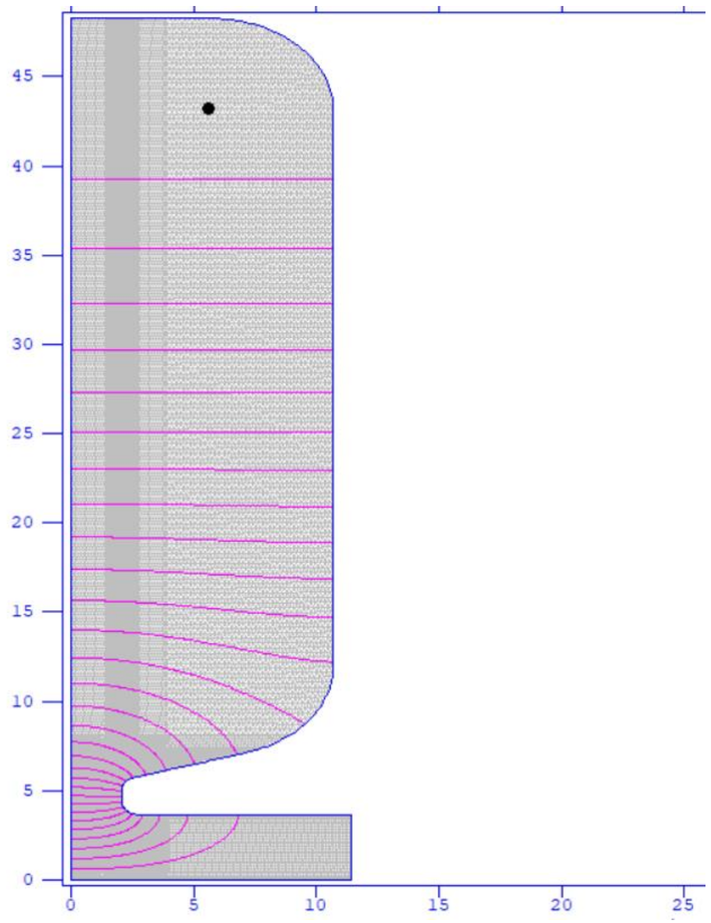

Magnet Design

Sam Leadley (samuel.leadley@physics.ox.ac.uk)
University of Oxford
Carl Jolly (carl.jolly@physics.ox.ac.uk)
University of Oxford

Magnet Design

Beam Parameters	
Energy	15 MeV
Momentum	0.168 GeV/c
Rigidity	0.561 Tm
Diameter	7.5 mm (1σ radius)

Magnet materials:
- Pure ***iron*** yokes
- ***Copper*** coils
- Vacuum/Air gaps

Good Field Region: 35mm (5σ radius)
Beam pipe radius: 50mm

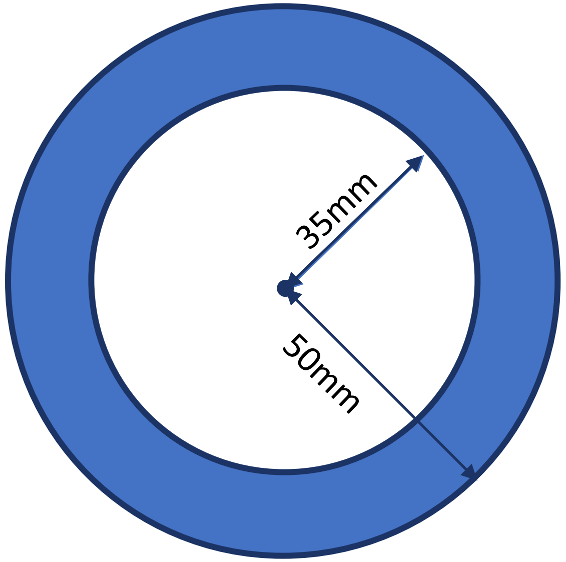

Required Magnets:

Vertical Arc Dipole:
Bending/beam ***selection*** into vertical arc

Vertical Arc Quadrupole:
Twiss manipulation and ***focusing*** in vertical arc

Extraction Octupole:
Flat beam profile

Nozzle Quadrupole:
Permanent magnet capturing beam after laser source

Magnetic Field Analysis

Polynomial Fit

$$B_y = \sum_{n=1}^{\infty} C_n x^{n-1}$$

Fit a curve to the absolute B-field value on a ***radial contour*** from the beamline to the edge of the beampipe.

Less accurate

- Monomial functions are ***not orthogonal***
- Fit depends on chosen monomials
- Easy to ***overfit*** data

Fourier Analysis

$$C_n = \frac{1}{M r_0^{n-1}} \sum_{m=0}^{M-1} B_m e^{-2\pi i n m/M}$$

Fourier transform of the B-field vector along an ***azimuthal contour*** around the Good Field Region of the beampipe.

More accurate

- Fourier coefficients are ***orthogonal***
- Fit is always the same
- Compare ***normal & skew*** components

Switching Dipole

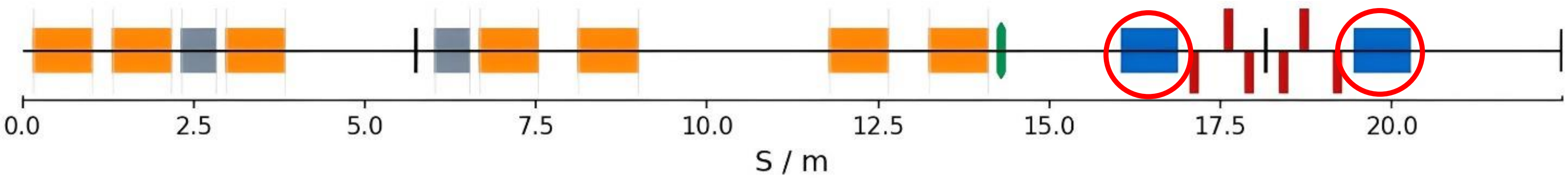

Initial requirements:

- $B_{gap} = 0.551$ T
- $B_{yoke} \leq 2.0$ T
- GFR field purity ≥ 99.9%

Coil Parameters	
Coil Area	20,000 mm^2
Current Density	0.93 Amm^{-2}
Turns	50
Cooling Method	Radiative

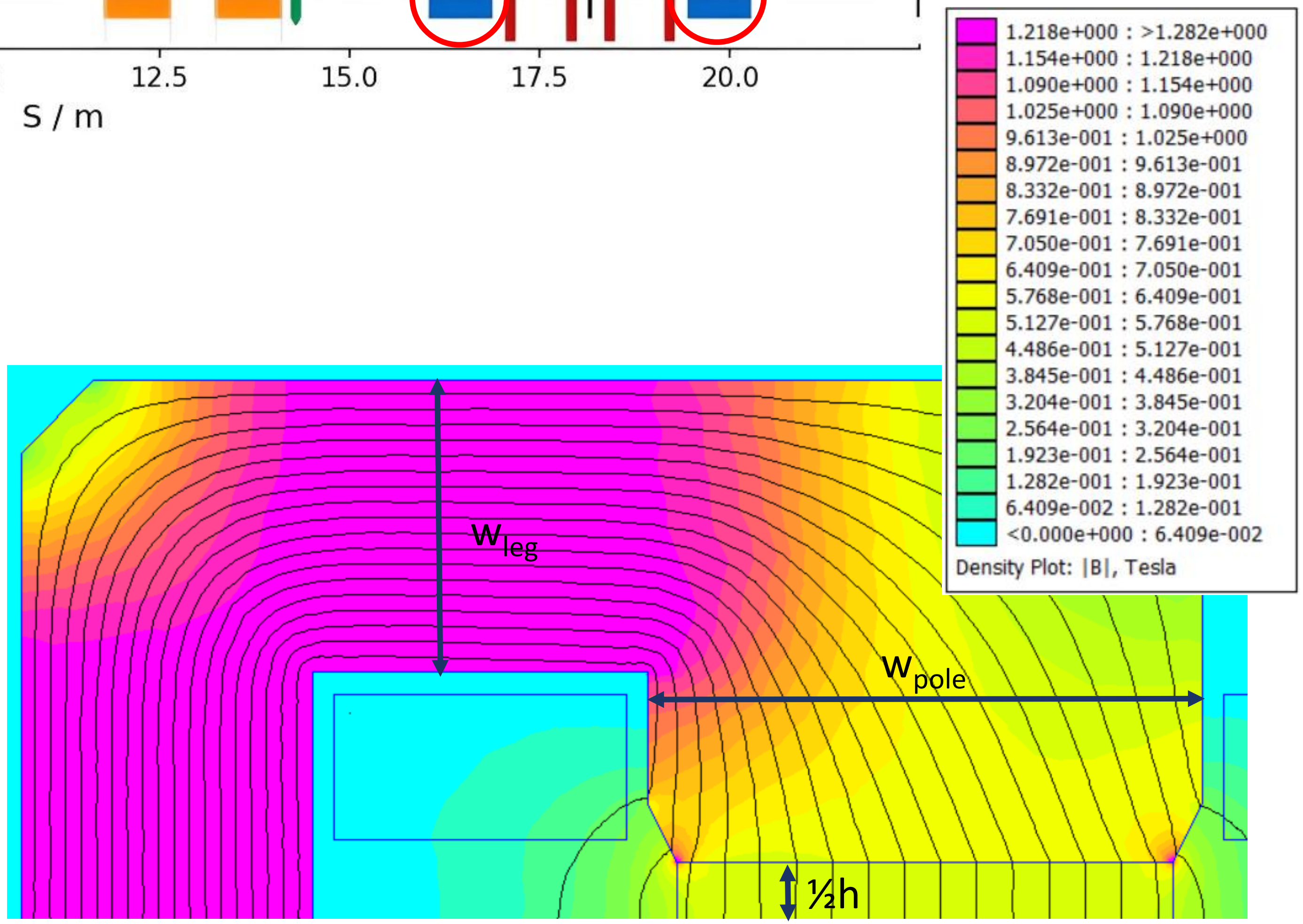

FEMM 4.2 output of ½-dipole magnet B-field, mesh size 0.03mm. C-shape for easy beam switching.

Magnet Design

Dipole GFR Field

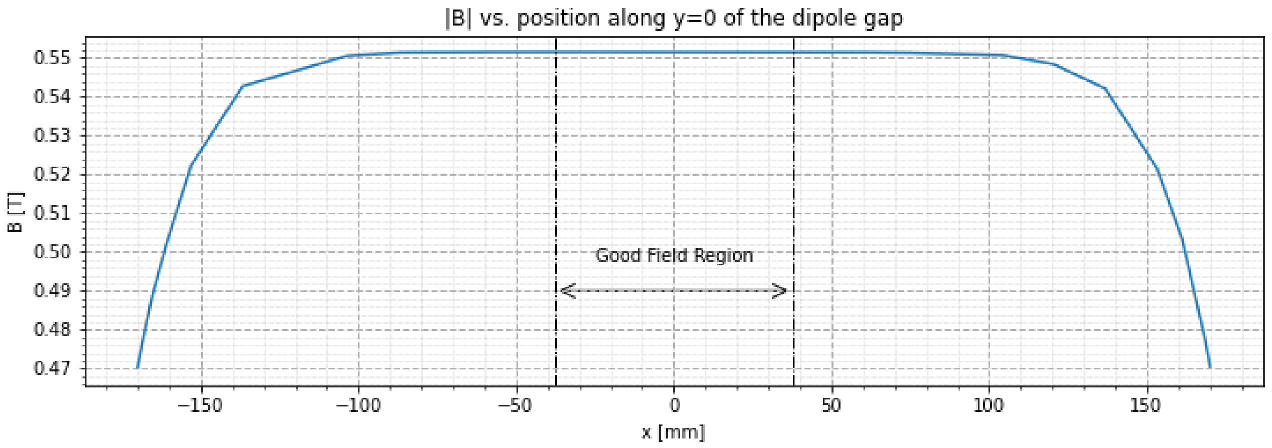

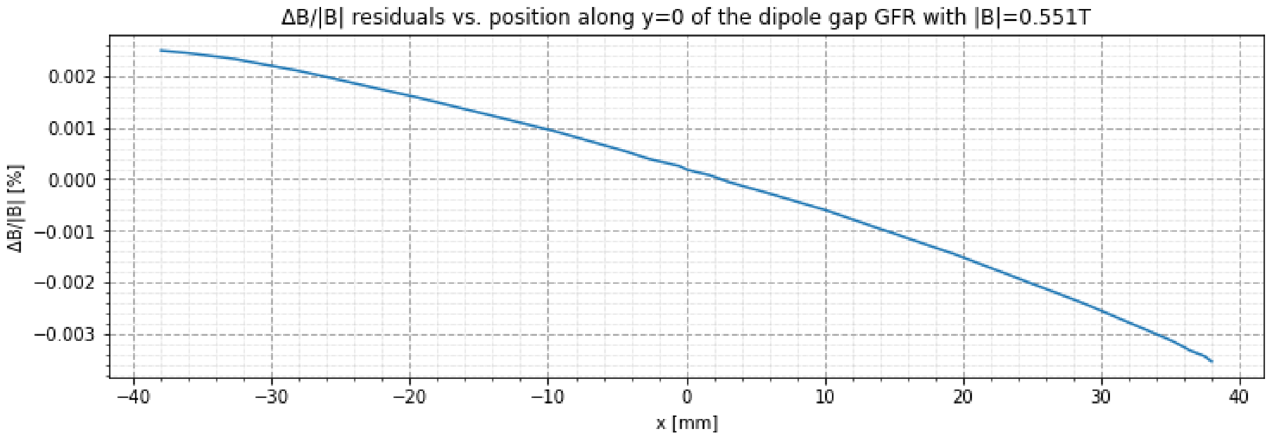

Simple fit takes **average B** across the **GFR** to assign a value to the field.

Standard dipole equations:

- $w_{pole}=w_{GFR}+2.5h$
- $B_{leg}=B_{gap}*(w_{pole}+1.2h)/w_{leg}$

Dipole Field Analysis

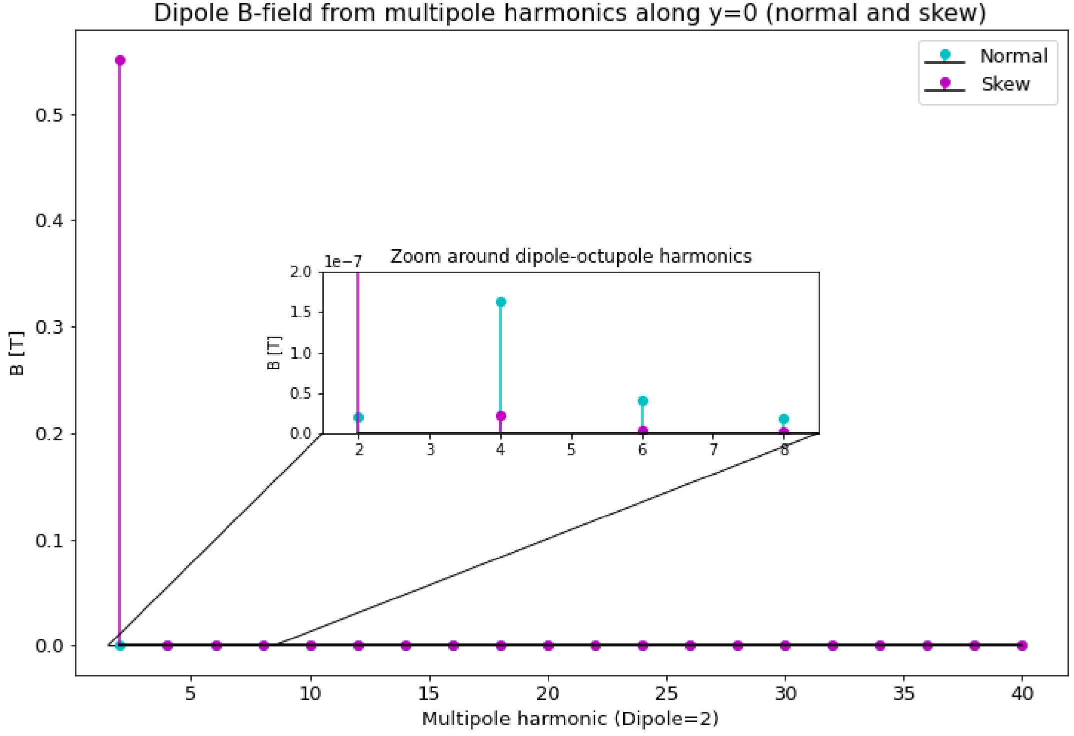

Harmonic	K-value (normal)	K-value (skew)	B@R=R_{GFR}
Dipole	**0.0 m^{-1}**	**0.551 m^{-1}**	**0.551 T**
Quadrupole	1.0×10^{-5} m^{-2}	*0.0 m^{-2}*	0.160 µT
Sextupole	1.2×10^{-4} m^{-3}	*1.0×10^{-5} m^{-3}*	0.041 µT
Octupole	4.5×10^{-3} m^{-4}	*2.9×10^{-4} m^{-4}*	0.018 µT
Decapole	0.291 m^{-5}	*0.0146 m^{-5}*	0.010 µT
Dodecapole	26.582 m^{-6}	*1.065 m^{-6}*	0.007 µT
14-pole (k6)	3165.3 m^{-7}	*107.93 m^{-7}*	0.005 µT
16-pole (k7)	4.7×10^{5} m^{-8}	*1.3×10^{4} m^{-8}*	0.003 µT

N.B. all values given are positive, no distinction is given to ±k
Main k in red bold, allowed harmonics in red italics.

Vertical Arc Quadrupole

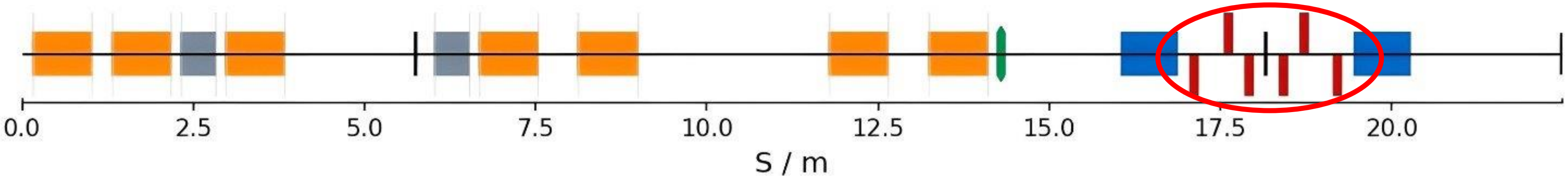

Initial requirements:

- $K_1 = 32.0\ m^{-2}$
- $B_{max} \leq 2.0$ T
- GFR field purity ≥ 99.9%

Coil Parameters	
Coil Area	4,070 mm^2
Current Density	5.31 Amm^{-2}
Turns	18
Cooling Method	Water cooled

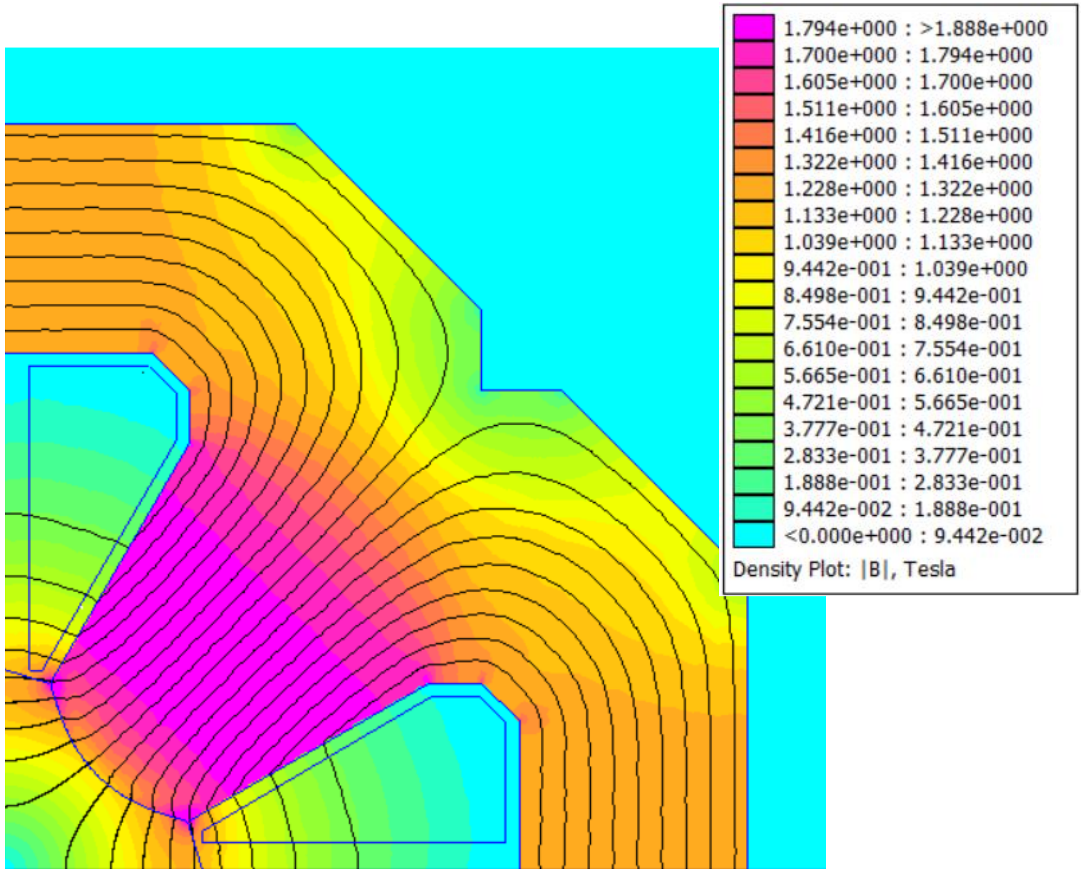

FEMM 4.2 output of ¼-quadrupole magnet B-field, mesh size 0.03mm

Magnet Design

Quadrupole GFR Field

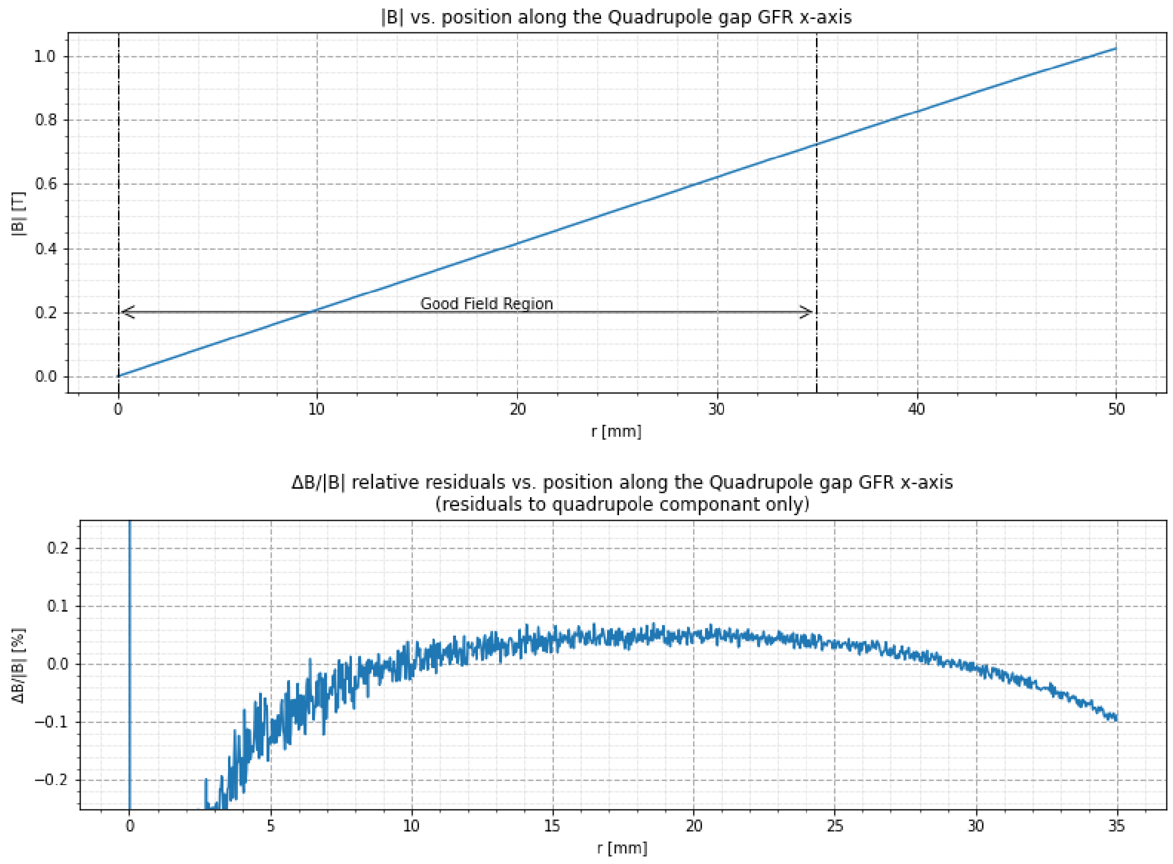

Quadrupole fitted with calculated $\mathbf{k_1 = 36.96m^{-2}}$

Residuals <0.1% for most of the GFR. Central part dominated by **mesh error** due to **small fields**

Quadrupole Field Analysis

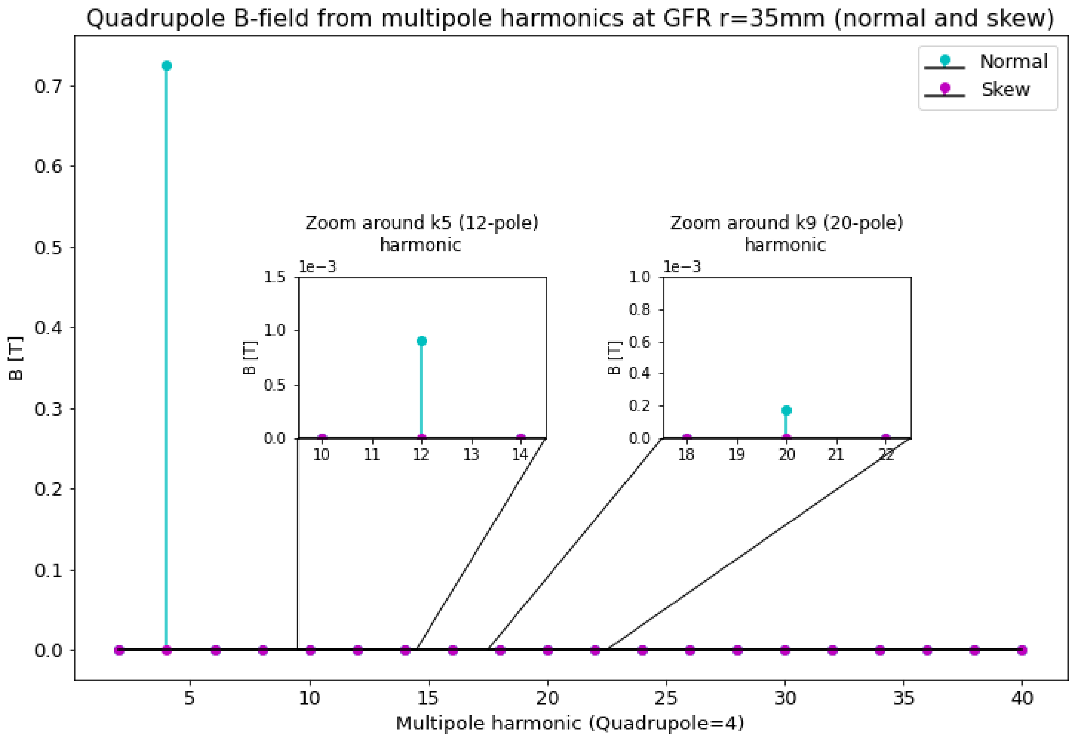

Harmonic	K-value (normal)	K-value (skew)	$B@R=R_{GFR}$
Dipole	$0.0\ m^{-1}$	$0.0\ m^{-1}$	0.0 T
Quadrupole	**$36.958\ m^{-2}$**	**$0.058\ m^{-2}$**	**0.726 T**
Sextupole	$0.0\ m^{-3}$	$0.0\ m^{-3}$	0.0 T
Octupole	$0.0\ m^{-4}$	$0.0\ m^{-4}$	0.0 T
Decapole	$0.0\ m^{-5}$	$0.0\ m^{-5}$	0.0 T
Dodecapole	*$3.7x10^{6}\ m^{-6}$*	$15,460\ m^{-6}$	0.908 mT
20-pole (k9)	*$1.4x10^{15}\ m^{-10}$*	$1.7x10^{13}\ m^{-10}$	0.174 mT
28-pole (k13)	*$3.7x10^{24}\ m^{-14}$*	$5.1x10^{22}\ m^{-14}$	0.039 mT

N.B. all values given are positive, no distinction is given to ±k.
Main k in red bold, allowed harmonics in red italics.

Extraction Octupole

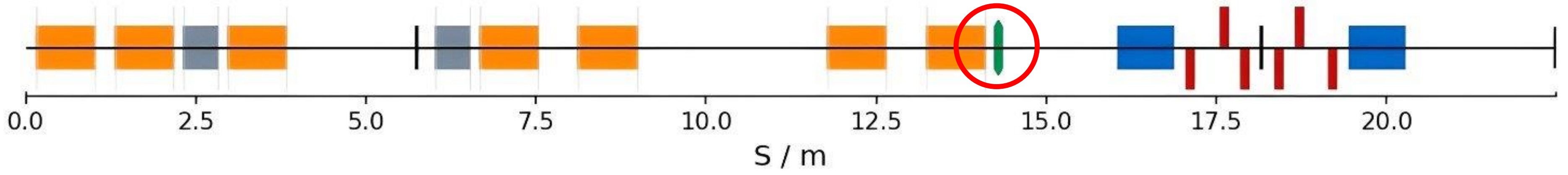

Initial requirements:

- $K_3 \geq 60{,}000\ m^{-4}$
- $B_{max} \leq 2.0$ T
- GFR field purity ≥ 99.9%

Coil Parameters	
Coil Area	3431 mm^2
Current Density	2.48 Amm^{-2}
Turns	10
Cooling Method	Water cooled

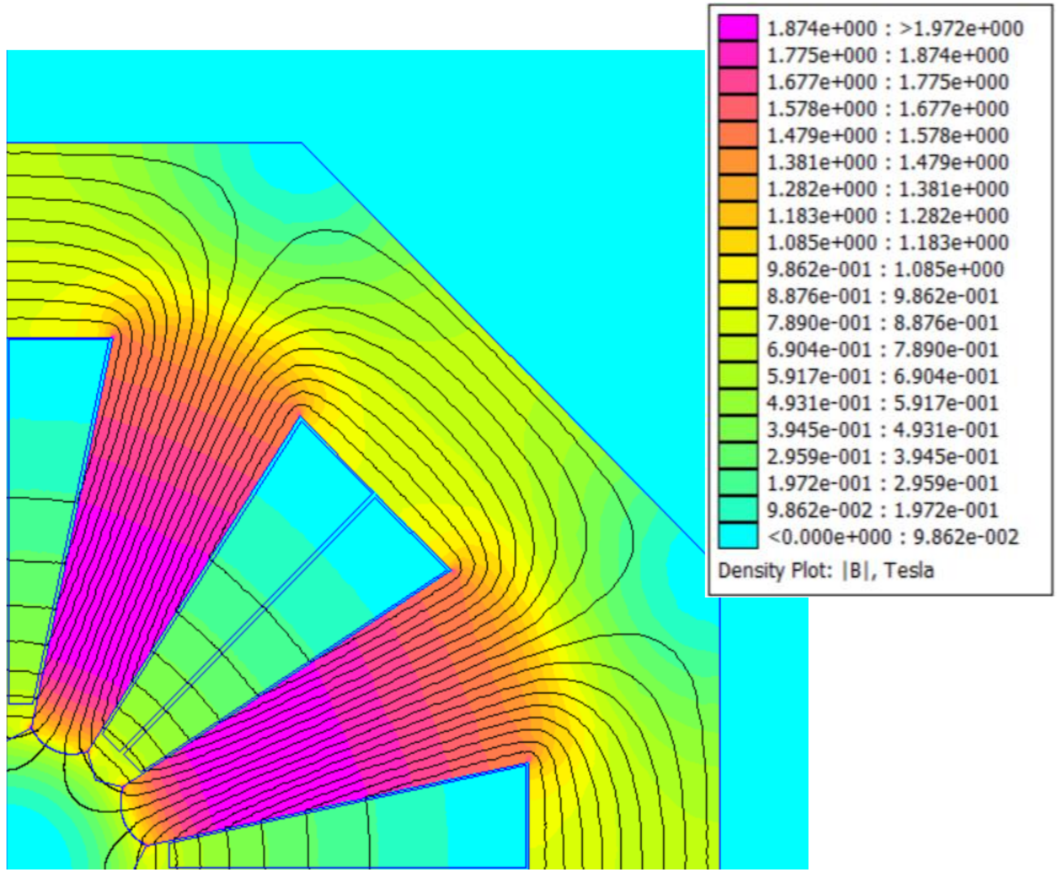

FEMM 4.2 output of ¼-octupole magnet B-field, mesh size 0.03mm

Magnet Design

Octupole GFR Field

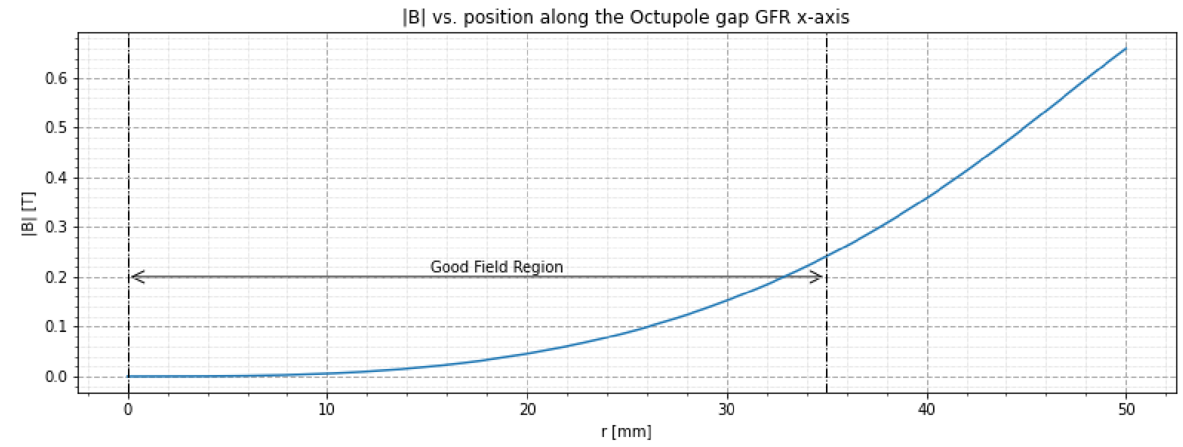

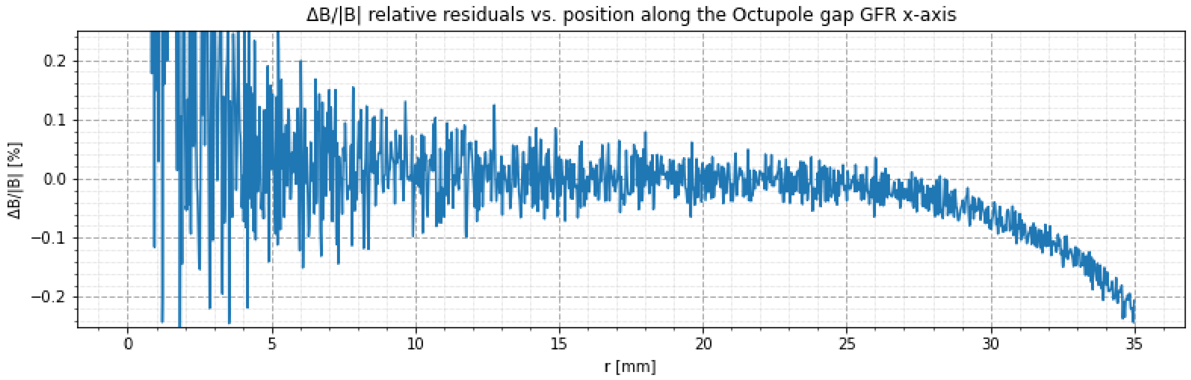

Octupole fitted with calculated **k_3 = 60273m^{-4}**

Relative **residuals <0.1%** up until edge of GFR (maximum 0.2%)

Octupole Field Analysis

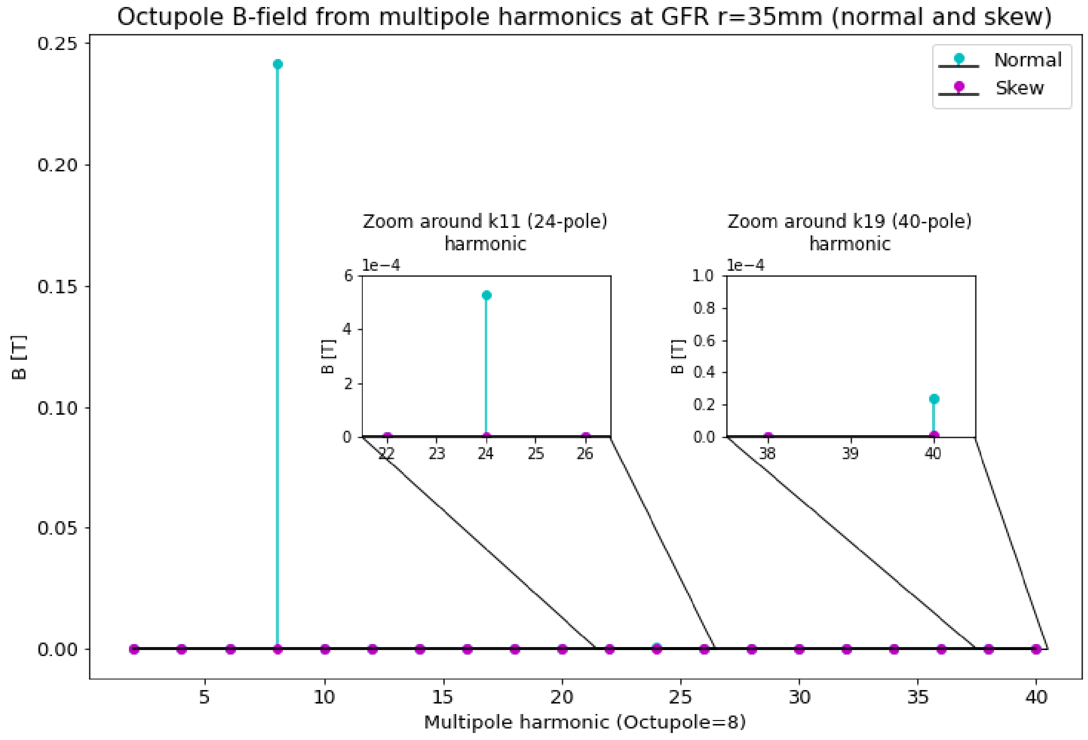

Harmonic	K-value (normal)	K-value (skew)	$B@R=R_{GFR}$
Dipole	$0.0\ m^{-1}$	$0.0\ m^{-1}$	0.0 T
Quadrupole	$0.0\ m^{-2}$	$0.0\ m^{-2}$	0.0 T
Sextupole	$0.0\ m^{-3}$	$0.0\ m^{-3}$	0.0 T
Octupole	**$60{,}273\ m^{-4}$**	**$0.1667\ m^{-4}$**	**0.242 T**
Decapole	$0.0\ m^{-5}$	$0.0\ m^{-5}$	0.0 T
Dodecapole	$0.0\ m^{-6}$	$0.0\ m^{-6}$	0.0 T
24-pole (k11)	*$3.9\times10^{20}\ m^{-12}$*	$2.4\times10^{17}\ m^{-12}$	0.527 mT
40-pole (k19)	*$2.4\times10^{40}\ m^{-20}$*	$7.9\times10^{38}\ m^{-20}$	0.024 mT

N.B. all values given are positive, no distinction is given to ±k
Main k in red bold, allowed harmonics in red italics.

Permanent Magnet Quadrupole Design

- Immediately after the laser ion/proton source the beam is extremely small leading to significant space charge effects.
- A focusing element at very near to the source could allow for more beam to be captured.
- The element must be small, high gradient and radiation hard....

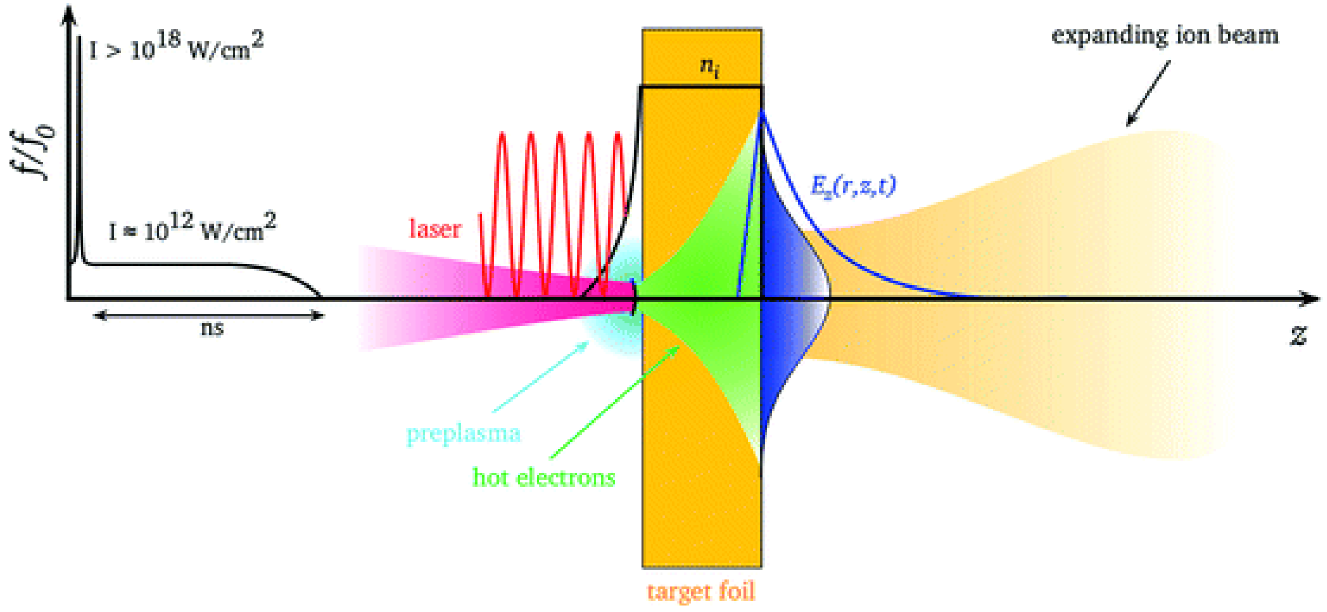

Permanent Magnet Quadrupole Design

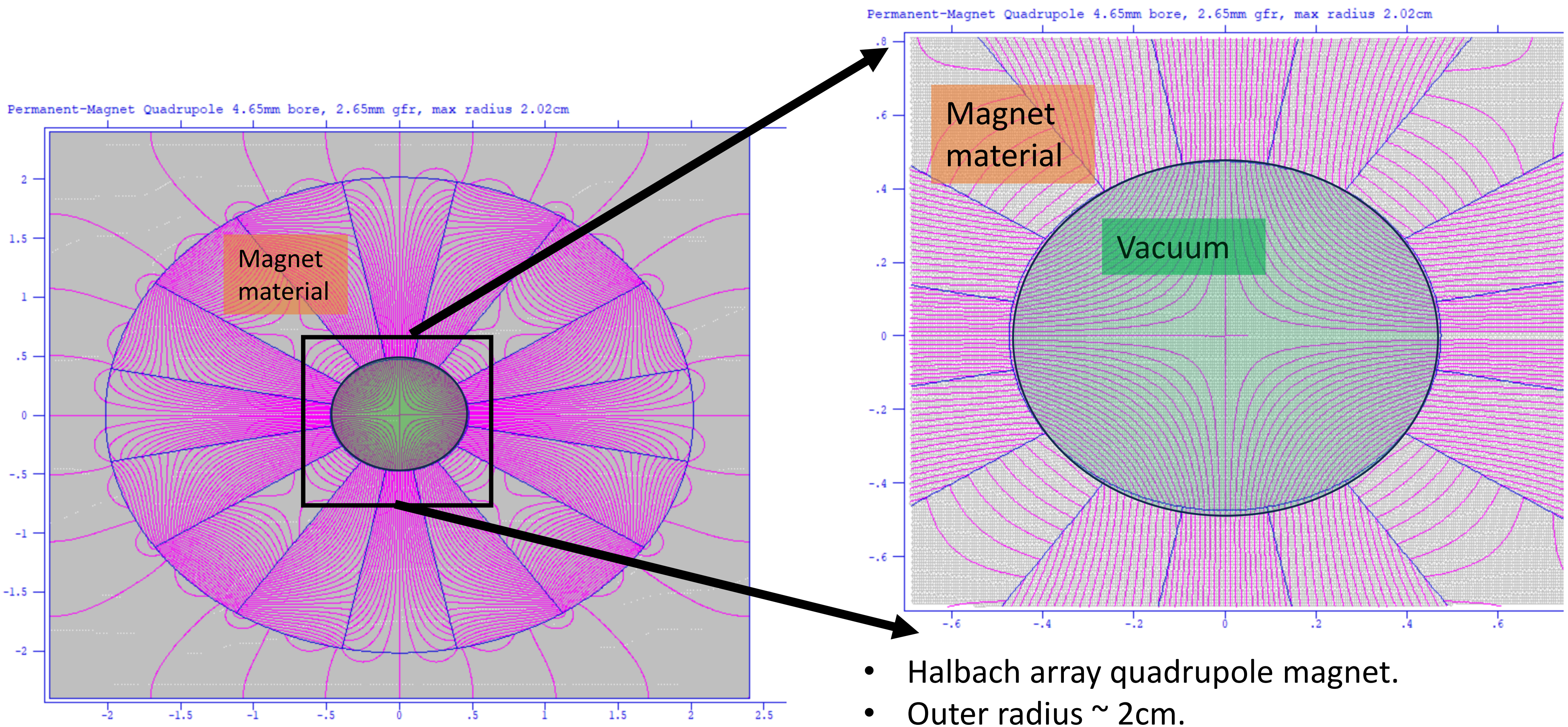

- Halbach array quadrupole magnet.
- Outer radius ~ 2cm.
- Samarium–cobalt magnet material.

Permanent Magnet Quadrupole Design

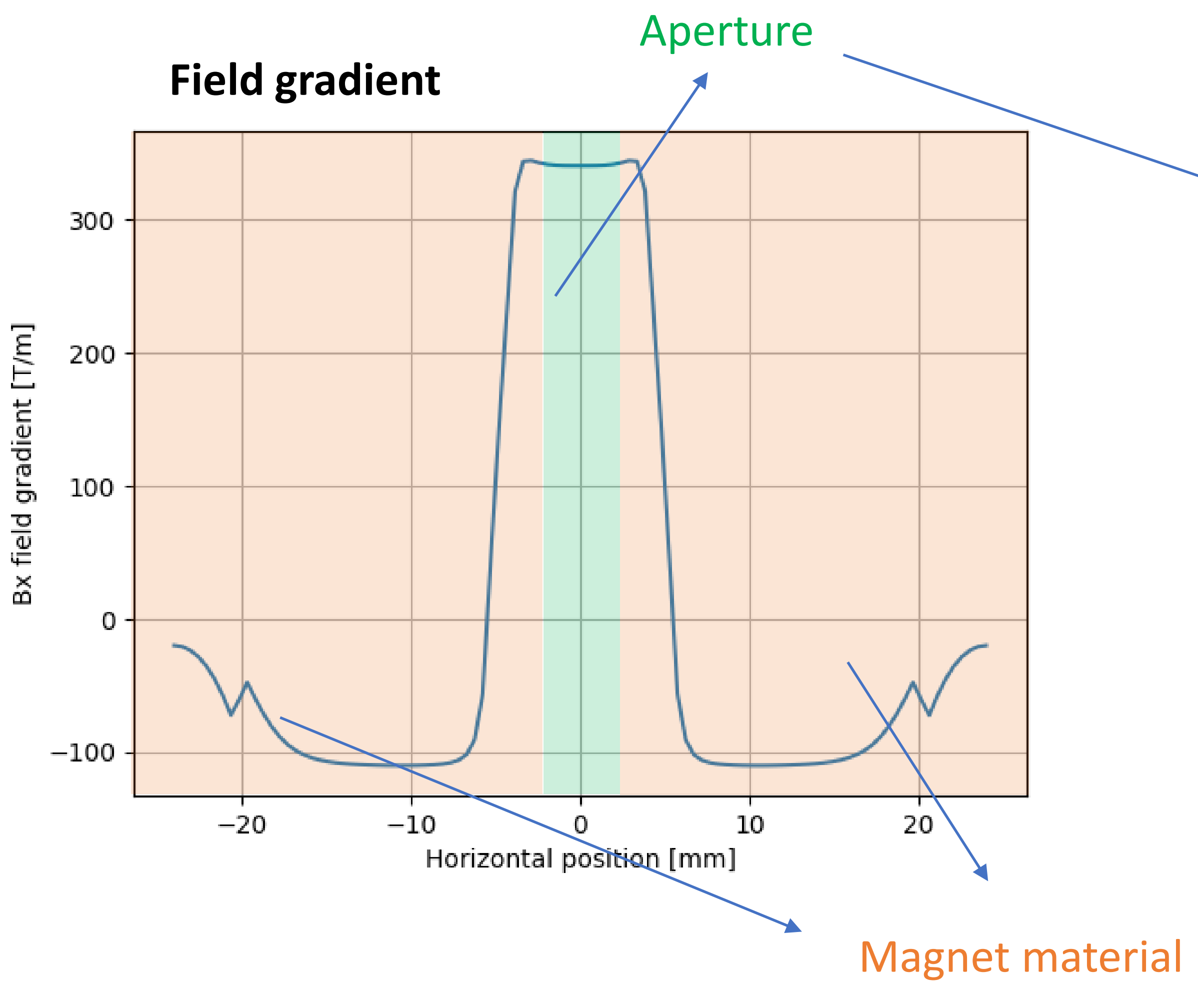

Summary

Lattice Design:
- Optimised configurations for spot sizes 3.0-1.0 cm
- Performance comparison between Gabor lenses and solenoids
- Quantified beam losses and end station dose rate
- Demonstrated the effect of the octupole on beam uniformity

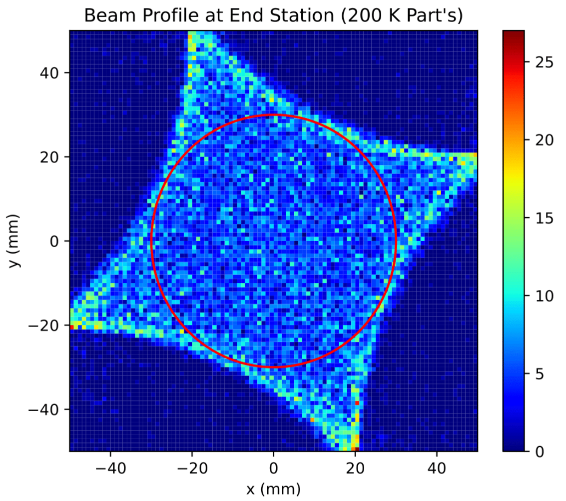

Cavity Design:
- 2D cavity geometry optimisation
- Particle tracking for bunching measurements
- 3D modelling using CST
- Phase-space comparison to BDSim

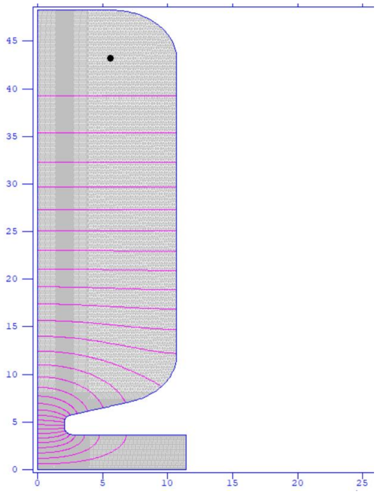

Magnet Design:
- 2D magnet design for dipoles, quadrupoles, octupole and PMQ
- Fourier harmonic analysis

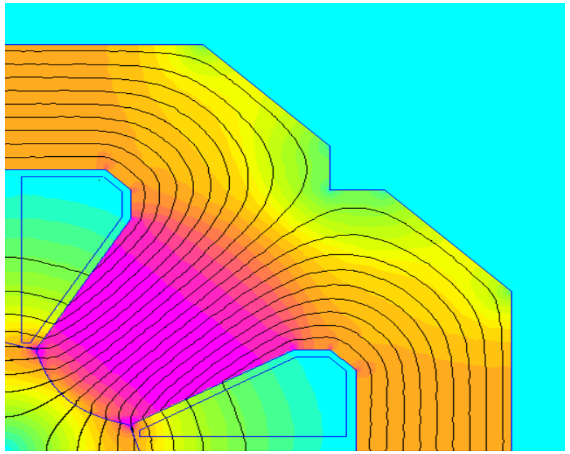

Bibliography

1. “Figure 1. Comparison of the Radiation Dose as Function of the Depth In...” ResearchGate, ResearchGate, 2020, www.researchgate.net/figure/Comparison-of-the-radiation-dose-as-function-of-the-depth-in-tissue-for-X-rays_fig5_230912423. Accessed 8 Mar. 2024.
2. Hageman, Eline, et al. “Radiobiological Aspects of FLASH Radiotherapy.” *Biomolecules*, vol. 12, no. 10, 26 Sept. 2022, pp. 1376–1376, www.mdpi.com/2218-273X/12/10/1376, https://doi.org/10.3390/biom12101376. Accessed 14 Mar. 2024.
3. Aymar, Galen, et al. “LhARA: The Laser-Hybrid Accelerator for Radiobiological Applications.” Frontiers in Physics, vol. 8, 29 Sept. 2020, www.frontiersin.org/articles/10.3389/fphy.2020.567738/full, https://doi.org/10.3389/fphy.2020.567738. Accessed 8 Mar. 2024.
4. “Figure 2.4: Target Normal Sheath Acceleration-TNSA. A Thin Target Foil...” ResearchGate, ResearchGate, 2016, www.researchgate.net/figure/Target-Normal-Sheath-Acceleration-TNSA-A-thin-target-foil-with-thickness-d-5-50_fig8_308718768. Accessed 8 Mar. 2024.
5. Gizzi, Leonida A, et al. “Enhanced Laser-Driven Proton Acceleration via Improved Fast Electron Heating in a Controlled Pre-Plasma.” *Scientific Reports*, vol. 11, no. 1, 2 July 2021, www.nature.com/articles/s41598-021-93011-3, https://doi.org/10.1038/s41598-021-93011-3. Accessed 14 Mar. 2024.
6. Palkovic, J.A., Mills, F.E., Schmidt, C., & Young, D.E. (1989). Gabor lens focusing of a negative ion beam (FNAL/C--89/115). United States
7. Kurup, A. & Long, K (2020) "LhARA: world-leading radiobiology and novel technology development" https://www.imperial.ac.uk/news/198093/lhara-world-leading-radiobiology-novel-technology-development/ Accessed 13 Mar. 2024.
8. L.J. Nevay et al., BDSIM: An Accelerator Tracking Code with Particle-Matter Interactions, Computer Physics Communications **252** 107200 (2020).
9. Powell, M.J.D. (1994). A Direct Search Optimization Method That Models the Objective and Constraint Functions by Linear Interpolation. In: Gomez, S., Hennart, JP. (eds) Advances in Optimization and Numerical Analysis. Mathematics and Its Applications, vol 275. Springer, Dordrecht. https://doi.org/10.1007/978-94-015-8330-5_4
10. D. C. Meeker, Finite Element Method Magnetics, Version 4.2 (28Feb2018 Build), https://ww.femm.info

MADX Matching and Optimisation

Varying Gabor Lens and Quadrupole strength to achieve smallest possible beam size

```
MATCH, SEQUENCE=lhara, betx=init_betx, bety=init_bety, alfx=init_alfx, alfy=init_alfy;
vary, name = LHA_LEL_MAG_QUAD_01->k1, step=1, lower=-33, upper=-15; // Vary k in gabor lens 4
vary, name = LHA_LEL_MAG_QUAD_02->k1, step=1, lower=10, upper=30; // Vary k in gabor lens 5
vary, name = LHA_LEL_MAG_QUAD_03->k1, step=1, lower=-33, upper=-15; // Vary k in gabor lens 6
vary, name = LHA_LEL_MAG_QUAD_04->k1, step=1, lower=-33, upper=-10; // Vary k in gabor lens 7
vary, name = LHA_LEL_MAG_QUAD_05->k1, step=1, lower=10, upper=33; // Vary k in gabor lens 7
vary, name = LHA_LEL_MAG_QUAD_06->k1, step=1, lower=-33, upper=-15; // Vary k in gabor lens 7
constraint, sequence=lhara, range = LHA_LEL_DIA_COL_04, dy>3.3; // Dispersion high in collimator
constraint, sequence=lhara, range = LHA_LEL_DIA_COL_04, bety<60; // Dispersion = 0 before arc
//constraint, sequence=lhara, range = LHA_LEL_DIA_COL_04, bety<60; // Dispersion = 0 before arc
constraint, sequence=lhara, range = LHA_LEL_VAC_DRI_30, bety<betaY; // Reduce Size at end station
constraint, sequence=lhara, range = LHA_LEL_VAC_DRI_30, betx<betaX; //^^^^^^^^^^
constraint, sequence=lhara, range = LHA_LEL_VAC_DRI_30, alfy=0; //Alfa 0 at end station
constraint, sequence=lhara, range = LHA_LEL_VAC_DRI_30, alfx=0;//^^^^^^^^^^
constraint, sequence=lhara, range = LHA_LEL_VAC_DRI_30, dy=0;// Dispersion = 0 at end station
constraint, sequence=lhara, range = LHA_LEL_VAC_DRI_30, dx=0;//^^^^^^^^^^
```

DOF

Constraints

Uses sum of squares of constraint functions